
CORE4D: A 4D Human-Object-Human Interaction Dataset for Collaborative Object REarrangement

Chengwen Zhang^{*1,2}, Yun Liu^{*1,3,4}, Ruofan Xing¹, Bingda Tang¹, Li Yi^{†1,3,4}

¹Institute for Interdisciplinary Information Sciences, Tsinghua University

²Beijing University of Posts and Telecommunications

³Shanghai Artificial Intelligence Laboratory

⁴Shanghai Qi Zhi Institute

zcwoctopus@gmail.com

{yun-liu22, xingrf20, tbd21}@mails.tsinghua.edu.cn

eric yi@mail.tsinghua.edu.cn

Abstract

Understanding how humans cooperatively rearrange household objects is critical for VR/AR and human-robot interaction. However, in-depth studies on modeling these behaviors are under-researched due to the lack of relevant datasets. We fill this gap by presenting CORE4D, a novel large-scale 4D human-object-human interaction dataset focusing on collaborative object rearrangement, which encompasses diverse compositions of various object geometries, collaboration modes, and 3D scenes. With 1K human-object-human motion sequences captured in the real world, we enrich CORE4D by contributing an iterative collaboration retargeting strategy to augment motions to a variety of novel objects. Leveraging this approach, CORE4D comprises a total of 11K collaboration sequences spanning 3K real and virtual object shapes. Benefiting from extensive motion patterns provided by CORE4D, we benchmark two tasks aiming at generating human-object interaction: human-object motion forecasting and interaction synthesis. Extensive experiments demonstrate the effectiveness of our collaboration retargeting strategy and indicate that CORE4D has posed new challenges to existing human-object interaction generation methodologies. Our dataset and code are available at <https://github.com/leolyliu/CORE4D-Instructions>.

1 Introduction

Humans frequently rearrange household items through multi-person collaboration, such as moving a table or picking up an overturned chair together. Analyzing and synthesizing these diverse collaborative behaviors could be widely applicable in VR/AR, human-robot interaction [77, 55, 54], and dexterous [10, 90, 76, 99] and humanoid [53, 18, 86, 42] manipulation. However, understanding and modeling these interactive motions have been under-researched due to the lack of large-scale, richly annotated datasets. Most existing human-object and hand-object interaction datasets focus on individual behaviors [71, 3, 49, 94, 20, 34, 100, 40, 46, 98] and two-person handovers [96, 81, 48]. But these datasets typically encompass a limited number of object instances, thus struggling to support generalizable interaction understanding across diverse object geometries. Scaling up precise human-object interaction data is challenging. While vision-based human-object motion tracking methods [3, 85] have made significant progress, they still struggle with low fidelity in severe occlusion, common in multi-human collaboration scenes. However, mocap [34, 40] is expensive and hard to scale up to cover a large number of objects to be rearranged. We want to curate a large-scale category-level human-object-human (HOH) interaction dataset with high motion quality in a cost-efficient manner.

*Equal contribution

†Corresponding author

We observe that HOH collaborations mainly vary in two aspects including the temporal collaboration patterns of two humans and the spatial relations between human and object. The temporal collaboration patterns could vary in many ways depending on scene complexity, motion range, and collaboration mode. In contrast, the spatial relations between human and object tend to possess strong homogeneity when facing objects from the same category, e.g., two persons holding the two sides of a chair. This allows retargeting interactions involving one specific instance to another using automatic algorithms, avoiding the need to capture interactions with thousands of same-category objects in the real world. The above observations make it possible for us to leverage expensive motion capture systems to capture only humans’ diverse temporal collaboration patterns while leaving the richness of human-object spatial relations to automatic spatial retargeting algorithms.

Using these insights, we build a large-scale dataset, CORE4D, encompassing a wide range of human-object interactions for collaborative object rearrangement. CORE4D includes various types of household objects, collaboration modes, and 3D environments. Our data acquisition strategy combines mocap-based capturing and synthetic retargeting, allowing us to scale the dataset effectively. The retargeting algorithm transfers spatial relation between human and object to novel object geometries while preserving temporal pattern of human collaboration. As a result, CORE4D includes 1K real-world motion sequences (CORE4D-Real) paired with videos and 3D scenes, and 10K synthetic collaboration sequences (CORE4D-Synthetic) covering 3K diverse object geometries.

We benchmark two tasks for generating human-object collaboration: (1) motion forecasting [12, 88] and (2) interaction synthesis [73, 40] on CORE4D, revealing challenges in modeling human behaviors, enhancing motion naturalness, and adapting to new object geometries. Ablation studies demonstrate the effectiveness of our hybrid data acquisition strategy, and the quality and value of CORE4D-Synthetic, highlighting its role in helping to improve existing motion generation methods.

In summary, our main contributions are threefold: (1) We present CORE4D, a large-scale 4D HOH interaction dataset for collaborative object rearrangement. (2) We propose a novel hybrid data acquisition methodology, incorporating real-world data capture and synthetically collaboration retargeting. (3) We benchmark two tasks for collaboration generation, revealing new challenges and research opportunities.

2 Related Work

2.1 Human-object Interaction Datasets

Tremendous progress has been made in constructing human-object interaction datasets. To study how humans interact with 3D scenes, various widely-used datasets record human movements and surrounding scenes separately, regarding objects as static [4, 66, 28, 80, 27, 44, 17, 102, 104, 26, 79, 2, 31, 91, 16, 25, 72, 92, 35, 97] or partially deformable [43] without pose changes. For dynamic objects, recent works [5, 71, 15, 3, 32, 34, 100, 40, 81, 48, 105, 101, 45] have captured human-object interaction behaviors with different focuses. Table 1 generally summarizes the characteristics of 4D human-object-interaction datasets. To support research for vision-based human-object motion tracking and shape reconstruction, a line of datasets [15, 3, 32, 34, 100, 105, 101, 45] presents human-object mesh annotations with multi-view RGB or RGBD signals. With the rapid development of human-robot cooperation, several works [5, 71, 81, 48] focus on specific action types such as grasping [71] and human-human handover [5, 81, 48]. Our dataset uniquely captures multi-person and object collaborative motions, category-level interactions, and both egocentric and allocentric views, offering comprehensive features with the inclusion of both real and synthetic datasets.

2.2 Human Interaction Retargeting

Human interaction retargeting focuses on how to apply human interactive motions to novel objects in human-object interaction scenarios. Existing methodologies [37, 65, 94, 67, 83, 8, 33] are object-centric, which propose first finding contact correspondences between the source and the target objects and then adjusting human motion to touch specific regions on the target object via optimization. As crucial guidance of the result, contact correspondences are discovered by aligning either surface regions [65, 94, 83], spatial maps [37, 33], distance fields [8], or neural descriptor fields [67] between the source and the target objects, which are all limited to objects with similar topology and scales. Our synthetic data generation strategy incorporates object-centric design [94] with novel human-centric contact selection, creating a chance to adapt to these challenging objects using human priors.

Table 1: Comparison of CORE4D with existing 4D human-object interaction datasets.

dataset	multi-human	collaboration	category-level	egocentric	RGBD	#view	mocap	#object	#sequence
<i>Carfi et.al.</i> [5]	✓				✓	1	✓	10	1.1K
GRAB [71]						-	✓	57	-
GraviCap [15]						3		4	9
BEHAVE [3]					✓	4		20	321
InterCap [32]					✓	6		10	223
CHAIRS [34]			✓		✓	4	✓	81	1.4K
HODome [100]						76	✓	23	274
<i>Li et.al.</i> [40]						-	✓	15	6.1K
HOH [81]	✓				✓	8		136	2.7K
CoChair [48]	✓		✓			-	✓	8	3.0K
FORCE [105]					✓	1	✓	8	450
HOI-M ³ [101]	✓					42	✓	90	199
CORE4D-Real	✓	✓	✓	✓	✓	5	✓	37	1.0K
CORE4D-Synthetic	✓	✓	✓			-	-	3.0K	10K

2.3 Human-object Interaction Generation

Human-object interaction generation is an emerging research topic that aims to synthesize realistic human-object motions conditioned on surrounding 3D scenes, known object trajectories, or action types. To generate humans interacting with static 3D scenes, POSA [29] and COINS [106] synthesize static human poses with CVAE [68], while a line of work [69, 22, 84, 70, 104, 38, 103] further presents dynamic human motions by auto-regressive manners [69, 104], diffusion models [38], or two-stage designs that first generates start and end poses and then interpolates motion in-between [22, 84, 70, 103]. InterDiff [88] and OMOMO [40] further fulfill this task for dynamic objects. To generate human-object interaction under specific action descriptions, recent works [19, 39, 63, 82, 89] extract text features with pretrained CLIP [64] encoders or LLMs [57, 74] and use them to guide diffusion models [30].

3 Constructing CORE4D

CORE4D is a large-scale 4D human-object-human interaction dataset acquired in a novel hybrid scheme, comprising CORE4D-Real and CORE4D-Synthetic. CORE4D-Real is captured (Section 3.1) and annotated (Section 3.2) from authentic collaborative scenarios. It provides human-object-human poses, allocentric RGB-D videos, egocentric RGB videos, and 2D segmentation across 1.0K sequences accompanied by 37 object models. To augment spacial relation between human and object, we present an innovative collaboration retargeting technique in Section 3.3, integrating CORE4D-Real with CORE4D-Synthetic, thereby expanding our collection with an additional 10K sequences and 3K rigid objects. Detailed characteristics such as data diversities are demonstrated in Section 3.4.

3.1 CORE4D-Real Data Capture

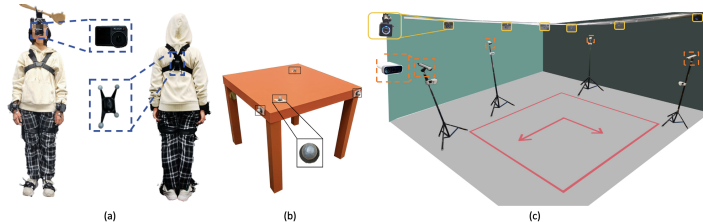


Figure 1: **Data capturing system.** (a) demonstrates the wearing of mocap suits and the positioning of the egocentric camera. (b) shows an object with four markers. (c) illustrates the data capturing system and camera views.

To collect precise human-object motions with visual signals, we set up a hybrid data capturing system shown in Fig. 1, consisting of an inertial-optical mocap system, four allocentric RGB-D cameras and a camera worn by persons for egocentric sensing. The frequency of our system is 15 FPS.

Inertial-optical Mocap System. To accurately capture human-object poses in multi-person collaboration scenarios, often involving severe occlusion, we use an inertial-optical mocap system [56] inspired by CHAIRS [34] This system includes 12 infrared cameras, mocap suits with 8 inertial-optical trackers and two data gloves per person, and markers of a 10mm radius. The mocap suits

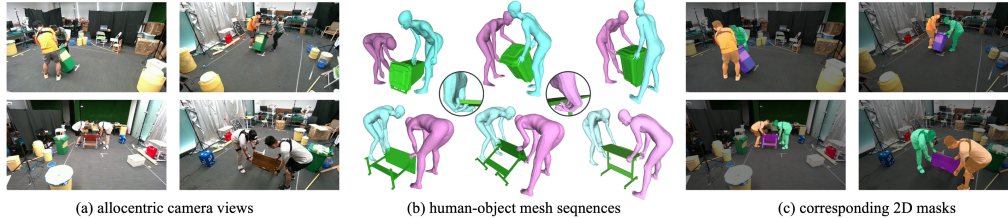


Figure 2: **Dataset overview.**

capture Biovision Hierarchy (BVH) skeletons of humans, while markers attached to the objects track object motion.

Visual Sensors. Kinect Azure DK cameras are integrated to capture allocentric RGB-D signals, and an Osmo Action3 is utilized to capture egocentric color videos. The resolution of all the visual signals is 1920x1080. Cameras are calibrated by the mocap system and synchronized via timestamp. Details on camera calibration and synchronization are provided in the supplementary material.

Object Model Acquisition. CORE4D-Real includes 37 3D models of rigid objects spanning six household object categories. Each object model is constructed by an industrial 3D scanner with up to 100K triangular faces. We additionally adopt manual refinements on captured object models to remove triangle outliers and improve accuracy.

Privacy Protection. To ensure participant anonymity, blurring is applied to faces [58] in RGB videos, and fake facial meshes are generated via SMPL-X [61]. The participants all consented to releasing CORE4D, and were also notified of their right to have their data removed from CORE4D at any time.

3.2 CORE4D-Real Data Annotation

Object Pose Tracking. To acquire the 6D pose of a rigid object, we attach four to five markers to the object’s surface. The markers formulate a virtual rigid that the mocap system can track. With accurate localization of the object manually, the object pose can be precisely determined by marker positions captured by the infrared cameras.

Human Mesh Acquisition. Aligning with existing dataset efforts [34, 40], we retarget the BVH [52] human skeleton to the widely-used SMPL-X [61]. SMPL-X [61] formulates a human mesh as $D_{\text{smplx}} = M(\beta, \theta)$. The body shape $\beta \in \mathbb{R}^{10}$ are optimized to fit the constraints on manually measured human skeleton lengths. With β computed, we optimize the full-body pose $\theta \in \mathbb{R}^{159}$ with the loss function:

$$\mathcal{L} = \mathcal{L}_{\text{reg}} + \mathcal{L}_{j3D} + \mathcal{L}_{j\text{Ori}} + \mathcal{L}_{\text{smooth}} + \mathcal{L}_{h3D} + \mathcal{L}_{h\text{Ori}} + \mathcal{L}_{\text{contact}}, \quad (1)$$

where \mathcal{L}_{reg} ensures the simplicity of the results and prevents unnatural, significant twisting of the joints. \mathcal{L}_{j3D} and $\mathcal{L}_{j\text{Ori}}$ encourage the rotation of joints and the global 3D positions to closely match the ground truth. \mathcal{L}_{h3D} and $\mathcal{L}_{h\text{Ori}}$ guide the positioning and orientation of the fingers. $\mathcal{L}_{\text{smooth}}$ promotes temporal smoothness. $\mathcal{L}_{\text{contact}}$ encourages realistic contact between the hands and objects. Then using SMPL-X [61] $M(\beta, \theta, \Phi) : \mathbb{R}^{|\theta| \times |\beta|} \mapsto \mathbb{R}^{3N}$ to generate human mesh. Details on the loss functions are presented in the supplementary material.

2D Mask Annotation. We offer automatic 2D segmentation for individuals and the manipulated object to aid in predictive tasks like vision-based human-object pose estimation [3, 85]. We first use DEVA [9] to segment human and object instances in a captured interaction image with text prompts. Then, we render human and object meshes separately on each image and select the instance with the highest Intersection-over-Union (IoU) for mask annotation.

3.3 CORE4D-Synthetic Data Generation

In order to enrich the diversities of object geometries and human-object spatial relations, our retargeting algorithm transfers real interactions to ShapeNet [6] objects of the same category, thereby significantly expanding the dataset regarding the object’s diversity. When transferring interactions across objects, contact points are always the key and it is important to consider whether they can be properly transferred with consistent semantics on new objects [95, 107]. However, we find this

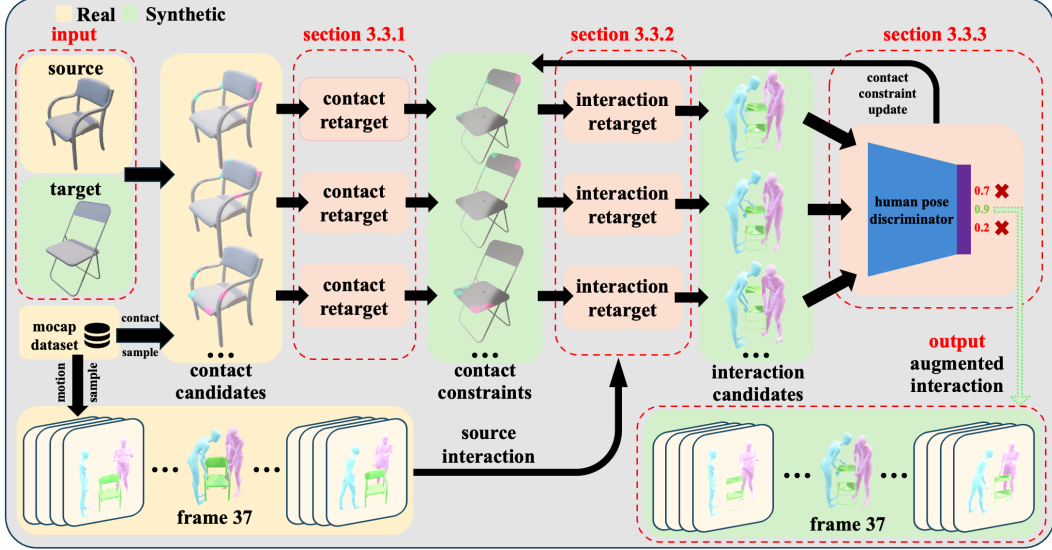


Figure 3: **Collaboration retargeting pipeline.** We propose a collaboration retargeting algorithm by iteratively refining interaction motion. The algorithm takes input *source-target* pair. First, we sample contact candidates from whole CORE4D-Real contact knowledge on *source*. For each contact candidate, we apply contact retargeting to propagate contact candidates to contact constraints on *target*. Sampled motion from CORE4D-Real provides a high-level collaboration pattern, together with low-level contact constraints, we obtain interaction candidates from interaction retargeting. Then, the human pose discriminator selects the optimal candidates, prompting a contact constraints update via beam search. After multiple iterations, the process yields augmented interactions. This iterative mechanism can effectively get a reasonable one from numerous contact constraints and ensures a refined interaction, enhancing the dataset’s applicability across various scenarios.

insufficient when object geometries vary largely and correspondences become hard to build. We thus tackle interaction retargeting from a novel human-centric perspective where good contact points should support natural human poses and motions. We realize this idea through the pipeline depicted in Figure 3, which comprises three key components. First, **object-centric contact retargeting** uses whole contact knowledge from CORE4D-Real to obtain accurate contact with different objects. Second, **contact-guided interaction retargeting** adapts motion sequences to new object geometries while considering the contact constraints. Third, a **human-centric contact selection** evaluates poses from interaction candidates to select the most plausible contacts.

Object-centric Contact Retargeting. To acquire reasonable human poses, contact constraints on the target object are essential. We draw inspiration from Tink [94] and train DeepSDF on all objects’ signed distance fields (SDFs). For *source* object SDF O_s and *target* object SDF O_t , we first apply linear interpolation on their latent vectors o_s and o_t and obtain N intermediate vectors $o_i = \frac{N+1-i}{N+1}o_s + \frac{i}{N+1}o_t (1 \leq i \leq N)$. We then decode o_i to its SDF O_i via the decoder of DeepSDF, and reconstruct the corresponding 3D mesh M_i using the Marching Cubes algorithm [50]. Thereby get mesh sequence $\mathcal{M} = [source, M_1, M_2, \dots, M_N, target]$ and successively transfer contact positions between every two adjacent meshes in \mathcal{M} via Nearest-neighbor searching. In addition, we leverage all contact candidates from CORE4D-Real on *source* to form a pool of contact candidates and transfer them to *target* as contact constraints.

Contact-guided Interaction Retargeting. For each contact constraint, interaction retargeting aims to transfer human interaction from *source* to *target*. To greatly enforce the consistency of interaction motion, we optimize variables including the object rotations $R_o \in \mathbb{R}^{N \times 3}$ and translations $T_o \in \mathbb{R}^{N \times 3}$, human poses $\theta_{1,2} \in \mathbb{R}^{2 \times N \times 153}$, translation $T_{1,2} \in \mathbb{R}^{2 \times N \times 3}$ and orientation $O_{1,2} \in \mathbb{R}^{2 \times N \times 3}$ on the SMPL-X [61]. N is the frame number.

We first estimate the *target*’s motion $\{R_o, T_o\}$ by solving an optimization problem as follows:

$$R_o, T_o \leftarrow \underset{R_o, T_o}{\operatorname{argmin}} (\mathcal{L}_f + \mathcal{L}_{\text{spat}} + \mathcal{L}_{\text{smooth}}), \quad (2)$$

where fidelity loss \mathcal{L}_f evaluates the difference of the *target*'s rotation and translation against the *source*, restriction loss $\mathcal{L}_{\text{spat}}$ penalizes *target*'s penetration with the ground, and smoothness loss $\mathcal{L}_{\text{smooth}}$ constrains the *target*'s velocities between consecutive frames.

Given the *target*'s motion and contact constraints, we then transfer humans' interactive motion $\{\theta_{1,2}, T_{1,2}, O_{1,2}\}$ from the *source* to the *target* by solving another optimization problem as follows:

$$\theta_{1,2}, T_{1,2}, O_{1,2} \leftarrow \underset{\theta_{1,2}, T_{1,2}, O_{1,2}}{\operatorname{argmin}} (\mathcal{L}_j + \mathcal{L}_c + \mathcal{L}_{\text{spat}} + \mathcal{L}_{\text{smooth}}), \quad (3)$$

where fidelity loss \mathcal{L}_j evaluates the difference in human joint positions before and after the transfer, contact loss \mathcal{L}_c computes the difference between human-object contact regions and the contact constraints, $\mathcal{L}_{\text{spat}}$ and $\mathcal{L}_{\text{smooth}}$ ensures the smoothness of human motion. Details on the loss designs and their motivations are provided in the supplementary material.

Human-centric Contact Selection. Selecting reasonable contact constraints efficiently is challenging due to their large scale and the time-consuming interaction retargeting. We address this challenge by developing a beam search algorithm to select contact constraints from a human-centric perspective. Specifically, we train a human pose discriminator inspired by GAN-based motion generation strategies [93, 87]. To train the discriminator, we build a pairwise training dataset, with each pair consisting of one positive human pose sample and one negative sample. Positive samples are encouraged to get higher scores than negative ones. We use CORE4D-Real as positive samples. We add 6D pose noise $\Delta(\alpha, \beta, \gamma, x, y, z)$ on *target* motion, and regard corresponding human motions generated by contact-guided interaction retargeting as negative samples. The loss function is:

$$\mathcal{L}_{\text{ranking}} = -\log(\sigma(R_{\text{pos}} - R_{\text{neg}} - m(S_{\text{pos}}, S_{\text{neg}}))), \quad (4)$$

where S_{pos} and S_{neg} denote inputs for positive and negative samples respectively, with R_{pos} and R_{neg} being their corresponding discriminator scores. σ is Sigmoid function, and $m(S_{\text{pos}}, S_{\text{neg}}) = \|\Delta(\alpha, \beta, \gamma, x, y, z)\|$ is human-guide margin [59] between positive and negative poses. This margin could explicitly instruct the discriminator to yield more significant disparities across different poses.

To ensure the realism of human interactions, we also introduce an interpenetration penalty. We prioritize those with the highest discriminator scores while ensuring acceptable levels of interpenetration as the optimal contact constraints.

3.4 Dataset Characteristics

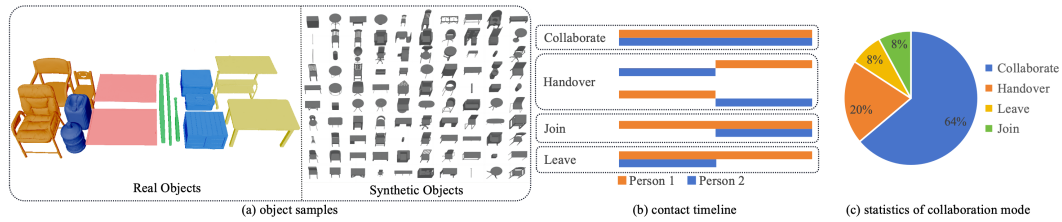


Figure 4: **Dataset statistics.** (a) shows some object samples from five categories. Bars in (b) indicate when the person is in contact with the object during the entire collaborative object rearrangement interaction process. (c) presents the proportion of collaboration modes in the dataset.

To better model collaborative object rearrangement interactions, we focus on diversifying our dataset in several vital areas: object geometries, collaboration modes, and 3D scenes. These ensure a comprehensive representation of real-world interactions.

Diversity in Object Geometries. We design six object categories to cover the main collaborative object rearrangement interaction scenarios as Fig. 4(a). Categories with relatively simple geometry, uniformity, and typically exhibiting symmetry include box, board, barrel, and stick. Categories with more complex geometries and significant individual differences include chair and desk.

Diversity in Collaboration Modes. We define five human-human collaboration modes in collaborative object rearrangement. Each mode represents a unique form of collaboration between two individuals, providing a new perspective and possibilities for understanding and researching collaborative behaviors. At first, we define the person with the egocentric camera as Person 2, and the other

Table 2: **Quantitative results on human-object motion forecasting.**

Test Set	Method	Human	Object			Contact	
		J_e (mm, ↓)	T_e (mm, ↓)	R_e (°, ↓)	C_{acc} (% , ↑)	P_r (% , ↓)	
S1	MDM [73]	170.8 (±0.9)	136.8 (±0.1)	10.7 (±0.1)	84.9 (± 0.2)	0.3 (± 0.0)	
	InterDiff [88]	170.8 (±0.9)	135.1 (±0.1)	10.2 (±0.1)	84.9 (± 0.2)	0.3 (± 0.0)	
	CAHMP [12]	169.4 (±0.3)	110.3 (±0.1)	9.0 (±0.1)	-	-	
S2	MDM [73]	186.4 (±0.7)	136.0 (±0.2)	11.1 (±0.0)	88.0 (± 0.0)	0.3 (± 0.0)	
	InterDiff [88]	186.4 (±0.7)	133.6 (±0.2)	10.7 (± 0.1)	88.0 (± 0.0)	0.3 (± 0.0)	
	CAHMP [12]	170.5 (±0.3)	112.9 (±0.1)	9.5 (±0.1)	-	-	

as Person 1. Collaborative carrying tasks are divided by whether Person 2 knows the goal or not. Tasks of handover and solely move alternate between the two participants. In join and leave tasks, Person 2 will either join in to help or leave halfway through, respectively.

Diversity in 3D Scenes. Surrounding scenarios are set up with varying levels of scene complexity: no obstacle, single obstacle, and many obstacles (more than one). Participants are asked to navigate through these randomly placed obstacles by their own means. We observe that this typically involved behaviors including bypassing, going through, stepping over, or moving obstacles aside.

4 Experiments

In this section, we first present the train-test split of CORE4D (Section 4.1). We then propose two benchmarks for generating human-object collaboration: human-object motion forecasting (Section 4.2), and interaction synthesis (Section 4.3). Finally, Section 4.4 presents extensive studies on the collaboration retargeting approach.

4.1 Data Split

We construct a training set from a random assortment of real objects, combining their real motions and corresponding synthetic data. We also create two test sets from CORE4D-Real for non-generalization and inner-category generalization studies. Test set S1 includes interactions with training set objects, while S2 features interactions with new objects. CORE4D-Synthetic is not included in the test set, avoiding potential biases from the retargeting algorithm. Details are shown in supplementary material.

4.2 Human-object Motion Forecasting

Forecasting 4D human motion [23, 62, 51, 24] is a crucial problem with applications in VR/AR and embodied perception [36]. Current research [13, 1, 77, 88] is limited to individual behaviors due to data constraints. Our work expands this by using diverse multi-person collaborations, making the prediction problem both intriguing and challenging.

Task Formulation. Given the object’s 3D model and human-object poses in adjacent 15 frames, the task is to predict their subsequent poses in the following 15 frames. The human pose $P_h \in \mathbb{R}^{23 \times 3}$ represents joint rotations of the SMPL-X [61] model, while the object pose $P_o = \{R_o \in \mathbb{R}^3, T_o \in \mathbb{R}^3\}$ denotes 3D orientation and 3D translation of the rigid object model.

Evaluation Metrics. Following existing motion forecasting works [12, 78, 88], we evaluate human joints position error J_e , object translation error T_e , object rotation error R_e , human-object contact accuracy C_{acc} , and penetration rate P_r . Details are provided in the supplementary material.

Methods, Results, and Analysis. We evaluate three state-of-the-art motion forecasting methods, MDM [73], InterDiff [88], and CAHMP [12]. Table 2 quantitatively shows these methods reveal a consistent drop in performance for unseen objects (S2) versus seen ones (S1) regarding human pose prediction. Meanwhile, errors in object pose prediction remain similar. This highlights the challenges in generalizing human collaborative motion for novel object shapes.

4.3 Interaction Synthesis

Generating human-object interaction [40, 19, 39, 63] is an emerging research topic benefiting human avatar animation and human-robot collaboration [11, 55]. With extensive collaboration modes

Table 3: **Quantitative results on interaction synthesis.**

Test Set	Method	$RR.J_e$ (mm, ↓)	$RR.V_e$ (mm, ↓)	C_{acc} (% , ↑)	FID (↓)
S1	MDM [73]	138.0 (± 0.3)	194.6 (± 0.2)	76.9 (± 0.5)	7.7 (± 0.2)
	OMOMO [40]	137.8 (± 0.2)	196.7 (± 0.3)	78.2 (± 0.5)	8.3 (± 0.6)
S2	MDM [73]	145.9 (± 0.2)	208.2 (± 0.2)	76.7 (± 0.1)	7.7 (± 0.2)
	OMOMO [40]	145.2 (± 0.6)	209.9 (± 1.0)	77.8 (± 0.3)	8.3 (± 1.0)

Table 4: **Ablation study.** CC denotes contact candidates. D denotes the human pose discriminator. CCU denotes the contact candidate update.

Comparisons		Designs			Penetration Distance (mm, ↓)	User Preferences	
		CC	D	CCU		Contact A/B/Approx.(%, ↑)	Motion A/B/Approx.(%, ↑)
Abl.1	A				6.06	7.8/88.9/3.3	3.3/84.4/12.3
	B	✓	✓		2.38		
Abl.2	A	✓			5.49	1.2/91.4/7.4	3.2/85.1/11.7
	B	✓	✓		2.38		
Abl.3	A	✓	✓		2.38	5.0/76.0/19.0	4.0/69.0/27.0
	B	✓	✓	✓	2.27		

and various object categories, CORE4D constitutes a knowledge base for studying generalizable algorithms of human-object-human interactive motion synthesis.

Task Formulation. Following recent studies [70, 40], we define the task as object-conditioned human motion generation. Given an object geometry sequence $G_o \in \mathbb{R}^{T \times N \times 3}$, the aim is to generate corresponding two-person collaboration motions $M_h \in \mathbb{R}^{2 \times T \times 23 \times 3}$. This involves frame numbers T , object point clouds G_o , and human pose parameters for the SMPL-X [61] model.

Evaluation Metrics. Following individual human-object interaction synthesis [40], we evaluate human joint position error $RR.J_e$, object vertex position error $RR.V_e$, and human-object contact accuracy C_{acc} . The FID score (FID) is leveraged to quantitatively assess the naturalness of synthesized results. Details of the metric designs are presented in the supplementary material.

Methods, Results, and Analysis. We utilize two advanced generative models, MDM [73] and OMOMO [40], as baselines. MDM is a one-stage conditional motion diffusion model, while OMOMO is a two-stage approach with hand positions as intermediate results. Quantitative evaluations reveal larger errors in OMOMO when modeling multi-human collaboration compared to individual interaction synthesis by *Li et al.* [40]. Furthermore, the synthesized results have a higher FID than real motion data, indicating challenges in motion naturalness.

4.4 Collaboration Retargeting

User Studies. We conduct user studies to examine the quality of CORE4D-Synthetic in terms of naturalness of contact and human motion. Each study comprises two collections, each with at least 100 sequences displayed in pairs on a website. Users are instructed to assess the realism of human-object contacts and the naturalness of human motions, and then select the superior one in each pair separately. Recognizing the diversity of acceptable contacts and motions, participants are permitted to deem the performances as roughly equivalent.

Ablation on Contact Candidates. In Table 4.Abl.1, we only use the contact points from a source trajectory for retargeting to the target instead of resorting to the CORE4D-Real for many candidates, making the whole retargeting process similar to the OakInk [94] method. We observe a sharp decline in both physical plausibility and user preferences, indicating that our method compensates for OakInk’s shortcomings in retargeting objects with significant geometric and scale variations.

Ablation on Discriminator. In this ablation, as shown in Table 4.Abl.2, we omit the human pose discriminator in the collaboration retargeting. We will randomly choose a candidate from the contact candidates. There are obvious performance drops, demonstrating the critical role of the human pose discriminator in selecting appropriate candidates.

Ablation on Contact Candidate Update. We exclude contact candidate update process in Table 4.Abl.3 experiment. This removal has weakened our method’s ability to search for optimal solutions

Table 5: Ablation on the incorporation of CORE4D-Synthetic on the motion forecasting task.

No	Train Set			Human	Object	
	Total	Real	Synthetic	J_e (mm, ↓)	T_e (mm, ↓)	R_e (°, ↓)
A	1.0K	0.1K	0.9K	127.7(± 0.7)	121.7(± 0.7)	8.04(± 0.4)
B	1.0K	1.0K	0	127.0(± 0.8)	120.5 (± 0.6)	9.48 (± 0.1)
C	5.0K	1.0K	4.0K	116.2(± 0.3)	112.1(± 0.2)	6.99(± 0.1)

on objects, resulting in a modest degradation in penetration distance. The user study still exhibited a strong bias, indicating a perceived decline in the plausibility of both contact and motion. This ablation underscores the importance of contact candidate update within our methodology.

Comparing CORE4D-Synthetic with CORE4D-Real. We assess the quality of CORE4D-Synthetic by comparing it with CORE4D-Real through user study. In conclusion, there is a 43% probability that users perceive the quality of both options as comparable. Furthermore, in 14% of cases, users even exhibit a preference for synthetic data. This indicates that the quality of our synthetic data closely approximates that of real data.

Application of CORE4D-Synthetic. Table 5 compares the motion forecasting ability of light-weighted CAHMP [14]. The test set is S2 defined in Section 4.1. We assess the quality of CORE4D-Synthetic by comparing No.A and No.B. No.A even have better performance on object due to enriched spacial relation between human and object in CORE4D-Synthetic. No.C shows the value of the CORE4D-Synthetic by largely improving the performance. Details are in supplementary material.

5 Conclusion and Limitations

We present CORE4D, a novel large-scale 4D human-object-human interaction dataset for collaborative object rearrangement. It comprises diverse compositions of various object geometries, collaboration modes, and surrounding 3D scenes. To efficiently enlarge the data scale, we contribute a hybrid data acquisition method involving real-world data capturing and a novel synthetic data augmentation algorithm, resulting in 11K motion sequences covering 37 real-world and 3K virtual objects. Extensive experiments demonstrate the effectiveness of the data augmentation strategy and the value of the augmented motion data. We benchmark human-object motion forecasting and interaction synthesis on CORE4D, revealing new challenges and research opportunities.

Limitations. One limitation is that outdoor scenes are not incorporated due to the usage of the mocap system. Another limitation is that our data augmentation strategy currently focuses on adopting collaboration to novel object geometries while excluding human shape diversity. Integrating our retargeting approach with human shape modeling could be an interesting future direction.

References

- [1] Adeli, V., Ehsanpour, M., Reid, I., Niebles, J.C., Savarese, S., Adeli, E., Rezatofghi, H.: Tripod: Human trajectory and pose dynamics forecasting in the wild. In: Proceedings of the IEEE/CVF International Conference on Computer Vision. pp. 13390–13400 (2021)
- [2] Araújo, J.P., Li, J., Vetrivel, K., Agarwal, R., Wu, J., Gopinath, D., Clegg, A.W., Liu, K.: Circle: Capture in rich contextual environments. In: Proceedings of the IEEE/CVF Conference on Computer Vision and Pattern Recognition. pp. 21211–21221 (2023)
- [3] Bhatnagar, B.L., Xie, X., Petrov, I.A., Sminchisescu, C., Theobalt, C., Pons-Moll, G.: Behave: Dataset and method for tracking human object interactions. In: Proceedings of the IEEE/CVF Conference on Computer Vision and Pattern Recognition. pp. 15935–15946 (2022)
- [4] Cao, Z., Gao, H., Mangalam, K., Cai, Q.Z., Vo, M., Malik, J.: Long-term human motion prediction with scene context. In: Computer Vision—ECCV 2020: 16th European Conference, Glasgow, UK, August 23–28, 2020, Proceedings, Part I 16. pp. 387–404. Springer (2020)
- [5] Carfi, A., Foglino, F., Bruno, B., Mastrogiovanni, F.: A multi-sensor dataset of human-human handover. *Data in brief* **22**, 109–117 (2019)
- [6] Chang, A.X., Funkhouser, T., Guibas, L., Hanrahan, P., Huang, Q., Li, Z., Savarese, S., Savva, M., Song, S., Su, H., et al.: Shapenet: An information-rich 3d model repository. *arXiv preprint arXiv:1512.03012* (2015)
- [7] Chao, Y.W., Yang, W., Xiang, Y., Molchanov, P., Handa, A., Tremblay, J., Narang, Y.S., Van Wyk, K., Iqbal, U., Birchfield, S., et al.: Dexycb: A benchmark for capturing hand grasping of objects. In: Proceedings of the IEEE/CVF Conference on Computer Vision and Pattern Recognition. pp. 9044–9053 (2021)
- [8] Chen, Z.Q., Van Wyk, K., Chao, Y.W., Yang, W., Mousavian, A., Gupta, A., Fox, D.: Learning robust real-world dexterous grasping policies via implicit shape augmentation. *arXiv preprint arXiv:2210.13638* (2022)
- [9] Cheng, H.K., Oh, S.W., Price, B., Schwing, A., Lee, J.Y.: Tracking anything with decoupled video segmentation. In: Proceedings of the IEEE/CVF International Conference on Computer Vision. pp. 1316–1326 (2023)
- [10] Christen, S., Kocabas, M., Aksan, E., Hwangbo, J., Song, J., Hilliges, O.: D-grasp: Physically plausible dynamic grasp synthesis for hand-object interactions. In: Proceedings of the IEEE/CVF Conference on Computer Vision and Pattern Recognition. pp. 20577–20586 (2022)
- [11] Christen, S., Yang, W., Pérez-D’Arpino, C., Hilliges, O., Fox, D., Chao, Y.W.: Learning human-to-robot handovers from point clouds. In: Proceedings of the IEEE/CVF Conference on Computer Vision and Pattern Recognition. pp. 9654–9664 (2023)
- [12] Corona, E., Pumarola, A., Alenya, G., Moreno-Noguer, F.: Context-aware human motion prediction. In: Proceedings of the IEEE/CVF Conference on Computer Vision and Pattern Recognition. pp. 6992–7001 (2020)
- [13] Corona, E., Pumarola, A., Alenya, G., Moreno-Noguer, F.: Context-aware human motion prediction. In: Proceedings of the IEEE/CVF Conference on Computer Vision and Pattern Recognition. pp. 6992–7001 (2020)
- [14] Corona, E., Pumarola, A., Alenyà, G., Moreno-Noguer, F.: Context-aware human motion prediction (2020)
- [15] Dabral, R., Shimada, S., Jain, A., Theobalt, C., Golyanik, V.: Gravity-aware monocular 3d human-object reconstruction. In: Proceedings of the IEEE/CVF International Conference on Computer Vision. pp. 12365–12374 (2021)
- [16] Dai, Y., Lin, Y., Lin, X., Wen, C., Xu, L., Yi, H., Shen, S., Ma, Y., Wang, C.: Sloper4d: A scene-aware dataset for global 4d human pose estimation in urban environments. In: Proceedings of the IEEE/CVF Conference on Computer Vision and Pattern Recognition. pp. 682–692 (2023)
- [17] Dai, Y., Lin, Y., Wen, C., Shen, S., Xu, L., Yu, J., Ma, Y., Wang, C.: Hsc4d: Human-centered 4d scene capture in large-scale indoor-outdoor space using wearable imus and lidar. In: Proceedings of the IEEE/CVF Conference on Computer Vision and Pattern Recognition. pp. 6792–6802 (2022)

- [18] Dao, J., Duan, H., Fern, A.: Sim-to-real learning for humanoid box loco-manipulation. arXiv preprint arXiv:2310.03191 (2023)
- [19] Diller, C., Dai, A.: Cg-hoi: Contact-guided 3d human-object interaction generation. arXiv preprint arXiv:2311.16097 (2023)
- [20] Fan, Z., Taheri, O., Tzionas, D., Kocabas, M., Kaufmann, M., Black, M.J., Hilliges, O.: Arctic: A dataset for dexterous bimanual hand-object manipulation. In: Proceedings of the IEEE/CVF Conference on Computer Vision and Pattern Recognition. pp. 12943–12954 (2023)
- [21] Geburu, T., Morgenstern, J., Vecchione, B., Vaughan, J.W., Wallach, H., Iii, H.D., Crawford, K.: Datasheets for datasets. *Communications of the ACM* **64**(12), 86–92 (2021)
- [22] Ghosh, A., Dabral, R., Golyanik, V., Theobalt, C., Slusallek, P.: Imos: Intent-driven full-body motion synthesis for human-object interactions. In: *Computer Graphics Forum*. vol. 42, pp. 1–12. Wiley Online Library (2023)
- [23] Guo, W., Bie, X., Alameda-Pineda, X., Moreno-Noguer, F.: Multi-person extreme motion prediction. In: Proceedings of the IEEE/CVF Conference on Computer Vision and Pattern Recognition. pp. 13053–13064 (2022)
- [24] Guo, W., Du, Y., Shen, X., Lepetit, V., Alameda-Pineda, X., Moreno-Noguer, F.: Back to mlp: A simple baseline for human motion prediction. In: Proceedings of the IEEE/CVF Winter Conference on Applications of Computer Vision. pp. 4809–4819 (2023)
- [25] Guzov, V., Chibane, J., Marin, R., He, Y., Sattler, T., Pons-Moll, G.: Interaction replica: Tracking human-object interaction and scene changes from human motion. arXiv preprint arXiv:2205.02830 (2022)
- [26] Guzov, V., Mir, A., Sattler, T., Pons-Moll, G.: Human positioning system (hps): 3d human pose estimation and self-localization in large scenes from body-mounted sensors. In: Proceedings of the IEEE/CVF Conference on Computer Vision and Pattern Recognition. pp. 4318–4329 (2021)
- [27] Hassan, M., Ceylan, D., Villegas, R., Saito, J., Yang, J., Zhou, Y., Black, M.J.: Stochastic scene-aware motion prediction. In: Proceedings of the IEEE/CVF International Conference on Computer Vision. pp. 11374–11384 (2021)
- [28] Hassan, M., Choutas, V., Tzionas, D., Black, M.J.: Resolving 3d human pose ambiguities with 3d scene constraints. In: Proceedings of the IEEE/CVF international conference on computer vision. pp. 2282–2292 (2019)
- [29] Hassan, M., Ghosh, P., Tesch, J., Tzionas, D., Black, M.J.: Populating 3d scenes by learning human-scene interaction. In: Proceedings of the IEEE/CVF Conference on Computer Vision and Pattern Recognition. pp. 14708–14718 (2021)
- [30] Ho, J., Jain, A., Abbeel, P.: Denoising diffusion probabilistic models. *Advances in neural information processing systems* **33**, 6840–6851 (2020)
- [31] Huang, C.H.P., Yi, H., Höschle, M., Safroshkin, M., Alexiadis, T., Polikovskiy, S., Scharstein, D., Black, M.J.: Capturing and inferring dense full-body human-scene contact. In: Proceedings of the IEEE/CVF Conference on Computer Vision and Pattern Recognition. pp. 13274–13285 (2022)
- [32] Huang, Y., Taheri, O., Black, M.J., Tzionas, D.: Intercap: Joint markerless 3d tracking of humans and objects in interaction. In: DAGM German Conference on Pattern Recognition. pp. 281–299. Springer (2022)
- [33] Huang, Z., Xu, H., Huang, H., Ma, C., Huang, H., Hu, R.: Spatial and surface correspondence field for interaction transfer. arXiv preprint arXiv:2405.03221 (2024)
- [34] Jiang, N., Liu, T., Cao, Z., Cui, J., Zhang, Z., Chen, Y., Wang, H., Zhu, Y., Huang, S.: Full-body articulated human-object interaction. In: Proceedings of the IEEE/CVF International Conference on Computer Vision. pp. 9365–9376 (2023)
- [35] Jiang, N., Zhang, Z., Li, H., Ma, X., Wang, Z., Chen, Y., Liu, T., Zhu, Y., Huang, S.: Scaling up dynamic human-scene interaction modeling. arXiv preprint arXiv:2403.08629 (2024)
- [36] Kasahara, S., Konno, K., Owaki, R., Nishi, T., Takeshita, A., Ito, T., Kasuga, S., Ushiba, J.: Malleable embodiment: changing sense of embodiment by spatial-temporal deformation of virtual human body. In: Proceedings of the 2017 CHI Conference on Human Factors in Computing Systems. pp. 6438–6448 (2017)

- [37] Kim, Y., Park, H., Bang, S., Lee, S.H.: Retargeting human-object interaction to virtual avatars. *IEEE transactions on visualization and computer graphics* **22**(11), 2405–2412 (2016)
- [38] Kulkarni, N., Rempe, D., Genova, K., Kundu, A., Johnson, J., Fouhey, D., Guibas, L.: Nifty: Neural object interaction fields for guided human motion synthesis. *arXiv preprint arXiv:2307.07511* (2023)
- [39] Li, J., Clegg, A., Mottaghi, R., Wu, J., Puig, X., Liu, C.K.: Controllable human-object interaction synthesis. *arXiv preprint arXiv:2312.03913* (2023)
- [40] Li, J., Wu, J., Liu, C.K.: Object motion guided human motion synthesis. *ACM Transactions on Graphics (TOG)* **42**(6), 1–11 (2023)
- [41] Li, J., Bian, S., Xu, C., Chen, Z., Yang, L., Lu, C.: Hybrik-x: Hybrid analytical-neural inverse kinematics for whole-body mesh recovery. *arXiv preprint arXiv:2304.05690* (2023)
- [42] Li, J., Nguyen, Q.: Kinodynamics-based pose optimization for humanoid loco-manipulation. *arXiv preprint arXiv:2303.04985* (2023)
- [43] Li, Z., Shimada, S., Schiele, B., Theobalt, C., Golyanik, V.: Mocapdeform: Monocular 3d human motion capture in deformable scenes. In: *2022 International Conference on 3D Vision (3DV)*. pp. 1–11. *IEEE* (2022)
- [44] Liu, M., Yang, D., Zhang, Y., Cui, Z., Rehg, J.M., Tang, S.: 4d human body capture from egocentric video via 3d scene grounding. In: *2021 international conference on 3D vision (3DV)*. pp. 930–939. *IEEE* (2021)
- [45] Liu, S., Li, Y.L., Fang, Z., Liu, X., You, Y., Lu, C.: Primitive-based 3d human-object interaction modelling and programming. In: *Proceedings of the AAAI Conference on Artificial Intelligence*. vol. 38, pp. 3711–3719 (2024)
- [46] Liu, Y., Yang, H., Si, X., Liu, L., Li, Z., Zhang, Y., Liu, Y., Yi, L.: Taco: Benchmarking generalizable bimanual tool-action-object understanding. In: *Proceedings of the IEEE/CVF Conference on Computer Vision and Pattern Recognition*. pp. 21740–21751 (2024)
- [47] Liu, Y., Yang, H., Si, X., Liu, L., Li, Z., Zhang, Y., Liu, Y., Yi, L.: Taco: Benchmarking generalizable bimanual tool-action-object understanding. *arXiv preprint arXiv:2401.08399* (2024)
- [48] Liu, Y., Chen, C., Yi, L.: Interactive humanoid: Online full-body motion reaction synthesis with social affordance canonicalization and forecasting. *arXiv preprint arXiv:2312.08983* (2023)
- [49] Liu, Y., Liu, Y., Jiang, C., Lyu, K., Wan, W., Shen, H., Liang, B., Fu, Z., Wang, H., Yi, L.: Hoi4d: A 4d egocentric dataset for category-level human-object interaction. In: *Proceedings of the IEEE/CVF Conference on Computer Vision and Pattern Recognition*. pp. 21013–21022 (2022)
- [50] Lorensen, W.E., Cline, H.E.: Marching cubes: A high resolution 3d surface construction algorithm. In: *Seminal graphics: pioneering efforts that shaped the field*, pp. 347–353 (1998)
- [51] Mao, W., Hartley, R.I., Salzmann, M., et al.: Contact-aware human motion forecasting. *Advances in Neural Information Processing Systems* **35**, 7356–7367 (2022)
- [52] Meredith, M., Maddock, S., et al.: Motion capture file formats explained. *Department of Computer Science, University of Sheffield* **211**, 241–244 (2001)
- [53] Murooka, M., Kumagai, I., Morisawa, M., Kanehiro, F., Kheddar, A.: Humanoid loco-manipulation planning based on graph search and reachability maps. *IEEE Robotics and Automation Letters* **6**(2), 1840–1847 (2021)
- [54] Ng, E., Liu, Z., Kennedy, M.: Diffusion co-policy for synergistic human-robot collaborative tasks. *IEEE Robotics and Automation Letters* (2023)
- [55] Ng, E., Liu, Z., Kennedy, M.: It takes two: Learning to plan for human-robot cooperative carrying. In: *2023 IEEE International Conference on Robotics and Automation (ICRA)*. pp. 7526–7532. *IEEE* (2023)
- [56] NOITOM INTERNATIONAL, INC: Noitom motion capture systems (2024), <https://www.noitom.com.cn/>
- [57] OpenAI: Chatgpt (2023), <https://chat.openai.com/>
- [58] OpenCV: opencv. https://github.com/opencv/opencv/blob/master/data/haarcascades/haarcascade_frontalface_default.xml (2013)

- [59] Ouyang, L., Wu, J., Jiang, X., Almeida, D., Wainwright, C., Mishkin, P., Zhang, C., Agarwal, S., Slama, K., Ray, A., et al.: Training language models to follow instructions with human feedback. *Advances in Neural Information Processing Systems* **35**, 27730–27744 (2022)
- [60] Park, J.J., Florence, P., Straub, J., Newcombe, R., Lovegrove, S.: Deepsdf: Learning continuous signed distance functions for shape representation. In: *Proceedings of the IEEE/CVF conference on computer vision and pattern recognition*. pp. 165–174 (2019)
- [61] Pavlakos, G., Choutas, V., Ghorbani, N., Bolkart, T., Osman, A.A., Tzionas, D., Black, M.J.: Expressive body capture: 3d hands, face, and body from a single image. In: *Proceedings of the IEEE/CVF conference on computer vision and pattern recognition*. pp. 10975–10985 (2019)
- [62] Peng, X., Shen, Y., Wang, H., Nie, B., Wang, Y., Wu, Z.: Somoforner: Social-aware motion transformer for multi-person motion prediction. *arXiv preprint arXiv:2208.09224* (2022)
- [63] Peng, X., Xie, Y., Wu, Z., Jampani, V., Sun, D., Jiang, H.: Hoi-diff: Text-driven synthesis of 3d human-object interactions using diffusion models. *arXiv preprint arXiv:2312.06553* (2023)
- [64] Radford, A., Kim, J.W., Hallacy, C., Ramesh, A., Goh, G., Agarwal, S., Sastry, G., Askell, A., Mishkin, P., Clark, J., et al.: Learning transferable visual models from natural language supervision. In: *International conference on machine learning*. pp. 8748–8763. PMLR (2021)
- [65] Rodriguez, D., Behnke, S.: Transferring category-based functional grasping skills by latent space non-rigid registration. *IEEE Robotics and Automation Letters* **3**(3), 2662–2669 (2018)
- [66] Savva, M., Chang, A.X., Hanrahan, P., Fisher, M., Nießner, M.: Pigraphs: learning interaction snapshots from observations. *ACM Transactions On Graphics (TOG)* **35**(4), 1–12 (2016)
- [67] Simeonov, A., Du, Y., Tagliasacchi, A., Tenenbaum, J.B., Rodriguez, A., Agrawal, P., Sitzmann, V.: Neural descriptor fields: Se (3)-equivariant object representations for manipulation. In: *2022 International Conference on Robotics and Automation (ICRA)*. pp. 6394–6400. IEEE (2022)
- [68] Sohn, K., Lee, H., Yan, X.: Learning structured output representation using deep conditional generative models. *Advances in neural information processing systems* **28** (2015)
- [69] Starke, S., Zhang, H., Komura, T., Saito, J.: Neural state machine for character-scene interactions. *ACM Trans. Graph.* **38**(6), 209–1 (2019)
- [70] Taheri, O., Choutas, V., Black, M.J., Tzionas, D.: Goal: Generating 4d whole-body motion for hand-object grasping. In: *Proceedings of the IEEE/CVF Conference on Computer Vision and Pattern Recognition*. pp. 13263–13273 (2022)
- [71] Taheri, O., Ghorbani, N., Black, M.J., Tzionas, D.: Grab: A dataset of whole-body human grasping of objects. In: *Computer Vision—ECCV 2020: 16th European Conference, Glasgow, UK, August 23–28, 2020, Proceedings, Part IV* 16. pp. 581–600. Springer (2020)
- [72] Tanke, J., Kwon, O.H., Mueller, F.B., Doering, A., Gall, J.: Humans in kitchens: A dataset for multi-person human motion forecasting with scene context. *Advances in Neural Information Processing Systems* **36** (2024)
- [73] Tevet, G., Raab, S., Gordon, B., Shafir, Y., Cohen-Or, D., Bermano, A.H.: Human motion diffusion model. *arXiv preprint arXiv:2209.14916* (2022)
- [74] Touvron, H., Martin, L., Stone, K., Albert, P., Almahairi, A., Babaei, Y., Bashlykov, N., Batra, S., Bhargava, P., Bhosale, S., et al.: Llama 2: Open foundation and fine-tuned chat models. *arXiv preprint arXiv:2307.09288* (2023)
- [75] Vaswani, A., Shazeer, N., Parmar, N., Uszkoreit, J., Jones, L., Gomez, A.N., Kaiser, Ł., Polosukhin, I.: Attention is all you need. *Advances in neural information processing systems* **30** (2017)
- [76] Wan, W., Geng, H., Liu, Y., Shan, Z., Yang, Y., Yi, L., Wang, H.: Unidexgrasp++: Improving dexterous grasping policy learning via geometry-aware curriculum and iterative generalist-specialist learning. In: *Proceedings of the IEEE/CVF International Conference on Computer Vision*. pp. 3891–3902 (2023)
- [77] Wan, W., Yang, L., Liu, L., Zhang, Z., Jia, R., Choi, Y.K., Pan, J., Theobalt, C., Komura, T., Wang, W.: Learn to predict how humans manipulate large-sized objects from interactive motions. *IEEE Robotics and Automation Letters* **7**(2), 4702–4709 (2022)

- [78] Wan, W., Yang, L., Liu, L., Zhang, Z., Jia, R., Choi, Y.K., Pan, J., Theobalt, C., Komura, T., Wang, W.: Learn to predict how humans manipulate large-sized objects from interactive motions. *IEEE Robotics and Automation Letters* **7**(2), 4702–4709 (2022)
- [79] Wang, Z., Chen, Y., Liu, T., Zhu, Y., Liang, W., Huang, S.: Humanise: Language-conditioned human motion generation in 3d scenes. *Advances in Neural Information Processing Systems* **35**, 14959–14971 (2022)
- [80] Wang, Z., Shin, D., Fowlkes, C.C.: Predicting camera viewpoint improves cross-dataset generalization for 3d human pose estimation. In: *Computer Vision–ECCV 2020 Workshops: Glasgow, UK, August 23–28, 2020, Proceedings, Part II* 16. pp. 523–540. Springer (2020)
- [81] Wiederhold, N., Megyeri, A., Paris, D., Banerjee, S., Banerjee, N.: Hoh: Markerless multimodal human-object-human handover dataset with large object count. *Advances in Neural Information Processing Systems* **36** (2024)
- [82] Wu, Q., Shi, Y., Huang, X., Yu, J., Xu, L., Wang, J.: Thor: Text to human-object interaction diffusion via relation intervention. *arXiv preprint arXiv:2403.11208* (2024)
- [83] Wu, R., Zhu, T., Peng, W., Hang, J., Sun, Y.: Functional grasp transfer across a category of objects from only one labeled instance. *IEEE Robotics and Automation Letters* **8**(5), 2748–2755 (2023)
- [84] Wu, Y., Wang, J., Zhang, Y., Zhang, S., Hilliges, O., Yu, F., Tang, S.: Saga: Stochastic whole-body grasping with contact. In: *European Conference on Computer Vision*. pp. 257–274. Springer (2022)
- [85] Xie, X., Bhatnagar, B.L., Pons-Moll, G.: Visibility aware human-object interaction tracking from single rgb camera. In: *Proceedings of the IEEE/CVF Conference on Computer Vision and Pattern Recognition*. pp. 4757–4768 (2023)
- [86] Xie, Z., Tseng, J., Starke, S., van de Panne, M., Liu, C.K.: Hierarchical planning and control for box loco-manipulation. *Proceedings of the ACM on Computer Graphics and Interactive Techniques* **6**(3), 1–18 (2023)
- [87] Xu, L., Song, Z., Wang, D., Su, J., Fang, Z., Ding, C., Gan, W., Yan, Y., Jin, X., Yang, X., et al.: Actformer: A gan-based transformer towards general action-conditioned 3d human motion generation. In: *Proceedings of the IEEE/CVF International Conference on Computer Vision*. pp. 2228–2238 (2023)
- [88] Xu, S., Li, Z., Wang, Y.X., Gui, L.Y.: Interdiff: Generating 3d human-object interactions with physics-informed diffusion. In: *Proceedings of the IEEE/CVF International Conference on Computer Vision*. pp. 14928–14940 (2023)
- [89] Xu, S., Wang, Z., Wang, Y.X., Gui, L.Y.: Interdreamer: Zero-shot text to 3d dynamic human-object interaction. *arXiv preprint arXiv:2403.19652* (2024)
- [90] Xu, Y., Wan, W., Zhang, J., Liu, H., Shan, Z., Shen, H., Wang, R., Geng, H., Weng, Y., Chen, J., et al.: Unidexgrasp: Universal robotic dexterous grasping via learning diverse proposal generation and goal-conditioned policy. In: *Proceedings of the IEEE/CVF Conference on Computer Vision and Pattern Recognition*. pp. 4737–4746 (2023)
- [91] Yan, M., Wang, X., Dai, Y., Shen, S., Wen, C., Xu, L., Ma, Y., Wang, C.: Cimi4d: A large multimodal climbing motion dataset under human-scene interactions. In: *Proceedings of the IEEE/CVF Conference on Computer Vision and Pattern Recognition*. pp. 12977–12988 (2023)
- [92] Yan, M., Zhang, Y., Cai, S., Fan, S., Lin, X., Dai, Y., Shen, S., Wen, C., Xu, L., Ma, Y., et al.: Reli1d: A comprehensive multimodal human motion dataset and method. *arXiv preprint arXiv:2403.19501* (2024)
- [93] Yan, S., Li, Z., Xiong, Y., Yan, H., Lin, D.: Convolutional sequence generation for skeleton-based action synthesis. In: *Proceedings of the IEEE/CVF International Conference on Computer Vision*. pp. 4394–4402 (2019)
- [94] Yang, L., Li, K., Zhan, X., Wu, F., Xu, A., Liu, L., Lu, C.: Oakink: A large-scale knowledge repository for understanding hand-object interaction. In: *Proceedings of the IEEE/CVF Conference on Computer Vision and Pattern Recognition*. pp. 20953–20962 (2022)
- [95] Yang, L., Zhan, X., Li, K., Xu, W., Li, J., Lu, C.: Cpf: Learning a contact potential field to model the hand-object interaction. In: *Proceedings of the IEEE/CVF International Conference on Computer Vision*. pp. 11097–11106 (2021)

- [96] Ye, R., Xu, W., Xue, Z., Tang, T., Wang, Y., Lu, C.: H2o: A benchmark for visual human-human object handover analysis. In: Proceedings of the IEEE/CVF International Conference on Computer Vision. pp. 15762–15771 (2021)
- [97] Yi, H., Thies, J., Black, M.J., Peng, X.B., Rempe, D.: Generating human interaction motions in scenes with text control. arXiv preprint arXiv:2404.10685 (2024)
- [98] Zhan, X., Yang, L., Zhao, Y., Mao, K., Xu, H., Lin, Z., Li, K., Lu, C.: Oakink2: A dataset of bimanual hands-object manipulation in complex task completion. In: Proceedings of the IEEE/CVF Conference on Computer Vision and Pattern Recognition. pp. 445–456 (2024)
- [99] Zhang, H., Christen, S., Fan, Z., Zheng, L., Hwangbo, J., Song, J., Hilliges, O.: Artigrasp: Physically plausible synthesis of bi-manual dexterous grasping and articulation. In: 2024 International Conference on 3D Vision (3DV). pp. 235–246. IEEE (2024)
- [100] Zhang, J., Luo, H., Yang, H., Xu, X., Wu, Q., Shi, Y., Yu, J., Xu, L., Wang, J.: Neurdome: A neural modeling pipeline on multi-view human-object interactions. In: Proceedings of the IEEE/CVF Conference on Computer Vision and Pattern Recognition. pp. 8834–8845 (2023)
- [101] Zhang, J., Zhang, J., Song, Z., Shi, Z., Zhao, C., Shi, Y., Yu, J., Xu, L., Wang, J.: Hoi-m3: Capture multiple humans and objects interaction within contextual environment. arXiv preprint arXiv:2404.00299 (2024)
- [102] Zhang, S., Ma, Q., Zhang, Y., Qian, Z., Kwon, T., Pollefeys, M., Bogo, F., Tang, S.: Egobody: Human body shape and motion of interacting people from head-mounted devices. In: European Conference on Computer Vision. pp. 180–200. Springer (2022)
- [103] Zhang, W., Dabral, R., Leimkühler, T., Golyanik, V., Habermann, M., Theobalt, C.: Roam: Robust and object-aware motion generation using neural pose descriptors. arXiv preprint arXiv:2308.12969 1 (2023)
- [104] Zhang, X., Bhatnagar, B.L., Starke, S., Guzov, V., Pons-Moll, G.: Couch: Towards controllable human-chair interactions. In: European Conference on Computer Vision. pp. 518–535. Springer (2022)
- [105] Zhang, X., Bhatnagar, B.L., Starke, S., Petrov, I., Guzov, V., Dhano, H., Pérez-Pellitero, E., Pons-Moll, G.: Force: Dataset and method for intuitive physics guided human-object interaction. arXiv preprint arXiv:2403.11237 (2024)
- [106] Zhao, K., Wang, S., Zhang, Y., Beeler, T., Tang, S.: Compositional human-scene interaction synthesis with semantic control. In: European Conference on Computer Vision. pp. 311–327. Springer (2022)
- [107] Zheng, J., Zheng, Q., Fang, L., Liu, Y., Yi, L.: Cams: Canonicalized manipulation spaces for category-level functional hand-object manipulation synthesis. In: Proceedings of the IEEE/CVF Conference on Computer Vision and Pattern Recognition. pp. 585–594 (2023)

Appendix

The project page of CORE4D is [CORE4D Project Page](#).

Contents:

- A. Cross-dataset Evaluation
- B. Details on Real-world Data Acquisition
- C. Details on CORE4D-Synthetic Data Generation
- D. Dataset Statistics and Visualization
- E. Details on Data Split
- F. Evaluation Metrics for Benchmarks
- G. Qualitative Results on Benchmarks
- H. Details on the Application of CORE4D-Synthetic
- I. CORE4D-Real Data Capturing Instructions and Costs
- J. Experiment Configurations and Codes
- K. URLs of Dataset, Repository, Metadata, DOI, and License
- L. Dataset Documentation and Intended Uses
- M. Author Statement

A Cross-dataset Evaluation

To examine the data quality of CORE4D-Real, we follow existing dataset efforts[91, 7, 47] and conduct the vision-based cross-dataset evaluation. We select an individual human-object-interaction dataset BEHAVE[3] that includes color images and select 2D human keypoint estimation as the evaluation task.

Data Preparation. For a color image from CORE4D-Real and BEHAVE[3], we first detect the bounding box for each person via ground truth human pose and obtain the image patch for the person. We then resize the image patch to get a maximal length of 256 pixels and fill it up into a 256x256 image with the black color as the background. Finally, for each 256x256 image, we automatically acquire the ground truth 2D-pixel coordinates of 22 SMPL-X[61] human body joints from 3D human poses. For data split, we follow the original train-test split for BEHAVE[3] and merge the two test sets (S1, S2) for CORE4D-Real.

Task Formulation. Given a 256x256 color image including a person, the task is to estimate the 2D-pixel coordinate for each of the 22 SMPL-X[61] human body joints.

Evaluation Metrics. P_e denotes the mean-square error of 2D coordinate estimates. Acc denotes the percentage of the coordinate estimates with the Euclidean distance to the ground truth smaller than 15 pixels.

Method, Results, and Analysis. We draw inspiration from HybrIK-X[41] and adopt their vision backbone as the solution. Table 6 shows the method performances on the two datasets under different training settings. Due to the significant domain gaps in visual patterns and human behaviors, transferring models trained on one dataset to the other would consistently encounter error increases. Despite the domain gaps, integrally training on both datasets achieves large performance gains on both CORE4D-Real and BEHAVE[3], indicating the accuracy of CORE4D-Real and the value of the dataset serving for visual perception studies.

B Details on Real-world Data Acquisition

In this section, we describe our system calibration (Section B.1) and time synchronization (Section B.2) in detail. Moreover, we provide detailed information on loss functions of the human mesh acquisition (Section B.3).

Table 6: **Cross-dataset evaluation with BEHAVE[3] on 2D human keypoint estimation.** Results are in P_e (pixel², lower is better) and Acc (% , higher is better), respectively.

Train \ Test	CORE4D-Real	BEHAVE[3]	CORE4D-Real + BEHAVE[3]
CORE4D-Real	152.4 / 91.2	904.9 / 35.6	121.7 / 92.4
BEHAVE[3]	887.9 / 37.8	146.3 / 88.9	128.2 / 89.8

B.1 System Calibration

Calibrating the Inertial-optical Mocap System. Three reflective markers are fixed at known positions on a calibration rod, by which the 12 high-speed motion capture cameras calculate their relative extrinsic parameters, providing information about their spatial relationships. Additionally, three markers fixed at the world coordinate origin are employed to calibrate the motion capture system coordinate with the defined world coordinate.

Calibrating Camera Intrinsic. The intrinsic parameters of allocentric and egocentric cameras are calibrated using a chessboard pattern.

Calibrating Extrinsic of the Allocentric Cameras. We place ten markers in the camera view to locate each allocentric camera. By annotating the markers’ 3D positions in the world coordinate system and their 2D-pixel coordinates on allocentric images, the camera’s extrinsic parameters are estimated by solving a Perspective-n-Point (PnP) problem via OpenCV.

Calibrating Extrinsic of the Egocentric Camera. We obtain the camera’s pose information by fixing the camera to the head tracker of the motion capture suit. Similarly, ten markers are used to calibrate the relative extrinsic parameters of the first-person perspective cameras, allowing for determining their positions and orientations relative to the motion capture system. Additionally, to mitigate errors introduced by the integration of optical and inertial tracking systems, a purely optical tracking rigid is mounted on the motion camera.

B.2 Time Synchronization

To implement our synchronization method, we first set up a Network Time Protocol (NTP) server on the motion capture host. This server serves as the time synchronization reference for the Windows computer connected to the Kinect Azure DK. We minimize time discrepancies by connecting the Windows computer to the NTP server in high-precision mode and thus achieving precise synchronization.

Additionally, we employ a Linear Timecode (LTC) generator to encode a time signal onto the action camera’s audio track. This time signal serves as a synchronization reference for aligning the first-person perspective RGB information with the motion capture data.

B.3 Loss Function Designs for Human Mesh Acquisition

To transfer the BVH[52] human skeleton to the widely-used SMPL-X[61] model. We optimize body shape parameters $\beta \in \mathbb{R}^{10}$ to fit the constraints on manually measured human skeleton lengths and then optimize the full-body pose $\theta \in \mathbb{R}^{159}$ with the following loss function:

$$\mathcal{L} = \mathcal{L}_{\text{reg}} + \mathcal{L}_{j3D} + \mathcal{L}_{j\text{Ori}} + \mathcal{L}_{\text{smooth}} + \mathcal{L}_{h3D} + \mathcal{L}_{h\text{Ori}} + \mathcal{L}_{\text{contact}}. \quad (5)$$

Regularization Loss \mathcal{L}_{reg} . The regularization loss term is defined as

$$\mathcal{L}_{\text{reg}} = \sum \|\theta_{\text{body}}\|^2 \cdot \lambda_{\text{body}} + \left(\sum \|\theta_{l_{\text{hand}}}\|^2 + \sum \|\theta_{r_{\text{hand}}}\|^2 \right) \cdot \lambda_{\text{hand}}, \quad (6)$$

where $\theta_{\text{body}} \in \mathbb{R}^{21 \times 3}$ represents the body pose parameters defined by 21 joints of the skeleton, $\theta_{l_{\text{hand}}} \in \mathbb{R}^{12}$ and $\theta_{r_{\text{hand}}} \in \mathbb{R}^{12}$ represents the hand pose parameters. For each hand, the original SMPL-X skeleton has 15 joints with parameters $\theta_{\text{hand}} \in \mathbb{R}^{15 \times 3}$. However, principal component analysis (PCA) is applied to the hand pose parameters. The θ_{hand} parameters are transformed into a lower-dimensional space, specifically \mathbb{R}^{12} . $\lambda_{\text{body}} = 10^{-3}$ and $\lambda_{\text{hand}} = 10^{-4}$ are different weights that are used to control the regularization strength for the body and hand pose parameters, respectively. This loss ensures the simplicity of the results and prevents unnatural, significant twisting of the joints.

3D Position Loss \mathcal{L}_{j3D} and \mathcal{L}_{h3D} . The 3D position loss term is defined as

$$\mathcal{L}_{3D} = \sum \|\mathbf{T}_{\text{smplx}} - \mathbf{T}_{\text{bvh}}\|^2 \cdot \lambda_{3D}, \quad (7)$$

where $\mathbf{T}_{\text{smplx}} \in \mathbb{R}^3$ represents the 3D global coordinates of the joints in the SMPL-X model and $\mathbf{T}_{\text{bvh}} \in \mathbb{R}^3$ represents the corresponding 3D global coordinates of the joints in the BVH representation. \mathcal{L}_{j3D} represents the 3D position loss sum for the 21 body joints, while \mathcal{L}_{h3D} represents the 3D position loss sum for the 30 hand joints (15 joints per hand). These two terms have different weights, set as $\lambda_{j3D} = 1.0$ and $\lambda_{h3D} = 2.0$, respectively.

Orientation Loss \mathcal{L}_{jOri} and \mathcal{L}_{hOri} . The orientation loss term is defined as

$$\mathcal{L}_{Ori} = \sum \|\mathbf{R}_{\text{smplx}} - \mathbf{R}_{\text{bvh}}\|^2 \cdot \lambda_{Ori}, \quad (8)$$

which is similar to \mathcal{L}_{3D} , except that $\mathcal{R}_{\text{smplx}} \in \mathbb{R}^{3 \times 3}$ and $\mathcal{R}_{\text{bvh}} \in \mathbb{R}^{3 \times 3}$ represent the rotation matrices for the adjacent joints in the SMPL-X and corresponding BVH representations, respectively. Specifically, body joints named head, spine, spine2, leftUpLeg, rightUpLeg, rightShoulder, leftShoulder, rightArm, leftArm, and neck are subjected to orientation loss, ensuring that their rotations relative to adjacent nodes are close to the BVH ground truth. λ_{Ori} is set to 0.2.

Temporal Smoothness Loss $\mathcal{L}_{\text{smooth}}$. The temporal smoothness loss term is defined as

$$\mathcal{L}_{\text{smooth}} = \sum_{i=1}^N \left(\|\theta_i - \theta_{i-1}\|^2 \right) \cdot \lambda_{\text{smooth}} \quad (9)$$

where $\theta_i \in \mathbb{R}^{(21+30) \times 3}$ represents the body and hand pose of the i -th frame. λ_{smooth} is set to 20.0.

Contact Loss $\mathcal{L}_{\text{contact}}$. The contact loss term is defined as

$$\mathcal{L}_{\text{contact}} = \sum \left(\|\mathbf{T}_{\text{finger}} - \mathbf{T}_{\text{obj}}\|^2 \cdot \mathcal{J}(\mathbf{T}_{\text{finger}}, \mathbf{T}_{\text{obj}}) \right) \cdot \lambda_{\text{contact}} \quad (10)$$

where $\mathcal{T}_{\text{finger}} \in \mathbb{R}^{10 \times 3}$ is the global coordinates of ten fingers, and $\mathcal{T}_{\text{obj}} \in \mathbb{R}^{10 \times 3}$ is the corresponding global coordinates of the point closest to finger. $\mathcal{J}(\mathbf{T}_{\text{finger}}, \mathbf{T}_{\text{obj}})$ is 1 when the distance between $\mathbf{T}_{\text{finger}}$ and \mathbf{T}_{obj} is less than a threshold, otherwise it is 0. And λ_{contact} is 2.0.

C Details on CORE4D-Synthetic Data Generation

In this section, we provide details on our synthetic data generation (collaboration retargeting) method. Firstly, we clarify term definitions in Section C.1. We then explicitly introduce the whole method pipeline in detail in Section C.2. Finally, we provide implementation details in Sections C.3 and C.4.

C.1 Term Definitions

We provide definitions for the terms in our collaboration retargeting pipeline as follows.

Contact Candidate: Contact candidate is a quadruple list containing all possible contact region index (person1_leftHand, person1_rightHand, person2_leftHand, person2_rightHand) on *source*'s vertices. For each *source*, we record the contact regions of the four hands in each frame of each data sequence. At the beginning of the synthetic data generation pipeline, we sample contact candidates from these records.

Contact Constraint: Having contact candidate on *source*, we apply DeepSDF-based[60] contact retargeting to transfer the contact regions to *target*. These contact regions on *target* are the contact constraints fed into the contact-guided interaction retargeting module.

Source Interaction: During each collaboration retargeting process, we sample a human-object-human collaborative motion sequence from CORE4D-Real as the source interaction to guide temporal collaboration pattern.

Interaction Candidate: Sampling N contact candidates, we apply contact-guided interaction retargeting N times and have N human-object-human motion outputs, dubbed interaction candidates. These motions would be fed into the human-centric contact selection module to assess their naturalness.

C.2 Method Pipeline

The algorithm takes a *source-target* pair as input. First, we sample contact candidates from the whole CORE4D-Real contact knowledge on *source*. For each contact candidate, we apply object-centric contact retargeting to propagate contact candidates to contact constraints on *target*. Sampling motion from CORE4D-Real provides a high-level temporal collaboration pattern, and together with augmented low-level spatial relations, we obtain interaction candidates from the contact-guided interaction retargeting. Then, the human-centric contact selection module selects the optimal candidates, prompting a contact constraint update. After multiple iterations, the process yields augmented interactions. This iterative mechanism ensures a refined augmentation of interactions, enhancing the dataset’s applicability across various scenarios.

C.3 Contact-guided Interaction Retargeting

The contact-guided interaction retargeting is a two-step optimization. We start by optimizing the motion of *target*. Then with *target* contact constraints, we optimize the poses of the two persons.

Object motion retargeting. We deliberately design temporal and spatial losses to acquire consistent and smooth *target* motion. In the concern of efficiency, we jointly optimize all frames in a single data sequence with N frames. To guarantee the fidelity of object motion, we design the fidelity loss \mathcal{L}_f to restrict the rotation $R_{o,i}$ and the translation $T_{o,i}$ with the ground-truth rotation $R'_{o,i}$ and translation $T'_{o,i}$ in N frames:

$$\mathcal{L}_f = \lambda_f \sum_i (\|R'_{o,i} - R_{o,i}\|_1 + \|T'_{o,i} - T_{o,i}\|_1). \quad (11)$$

We then address restriction on *target*’s spatial position to avoid penetration with the ground. The spatial loss is defined as:

$$\mathcal{L}_{\text{spat}} = \lambda_{\text{spat}} \sum_i \max(-\min(\text{height}_i), 0), \quad (12)$$

where $\min(\text{height}_i)$ represents the lowest spatial position of the objects per frame. A smoothness loss is designed to constrain the object pose difference between consecutive frames:

$$\mathcal{L}_{\text{smooth}} = \lambda_{\text{smooth}} \sum_i a_{R_{o,i}}^2 + a_{T_{o,i}}^2, \quad (13)$$

where a is the acceleration of rotation and translation during N frames defined as:

$$a_{R_{o,i}} = 2R_{o,i} - R_{o,i-1} - R_{o,i+1}, \quad (14)$$

$$a_{T_{o,i}} = 2T_{o,i} - T_{o,i-1} - T_{o,i+1}, \quad (15)$$

The total object motion retargeting problem is:

$$R_o, T_o \leftarrow \underset{R_o, T_o}{\operatorname{argmin}} (\mathcal{L}_f + \mathcal{L}_{\text{spat}} + \mathcal{L}_{\text{smooth}}). \quad (16)$$

Human motion retargeting. We next optimize each person’s motion based on the motion of *target* and the contact constraint. To acquire visually plausible motion, we design the fidelity loss \mathcal{L}_j and the smoothness loss $\mathcal{L}_{\text{smooth}}$. Besides, we utilize the contact correctness loss \mathcal{L}_c to acquire contact consistency in *target* interaction motion, and leverage spatial loss $\mathcal{L}_{\text{spat}}$ similar to Equation 12 to avoid human-ground inter-penetration.

To enhance motion fidelity, we define two loss functions \mathcal{L}_{sr} and \mathcal{L}_{wr} and let $L_j = \mathcal{L}_{\text{sr}} + \mathcal{L}_{\text{wr}}$. For joints from the human arms, despite following the correct temporal collaboration pattern, their global positions would vary concerning diverse object geometries. Therefore, we utilize oriented vectors pointing to their parent body joints to obtain a relative joint fidelity:

$$\mathcal{L}_{\text{sr}} = \lambda_{\text{sr}} \sum_i \sum_{j \in \text{arm}} \|(P_{j,i} - P_{\text{parent}(j),i}) - (P'_{j,i} - P'_{\text{parent}(j),i})\|_2^2, \quad (17)$$

where $P_{j,i}$ denotes the 3D global position of joint j in frame i , and P' denotes ground-truth values. \mathcal{L}_{wr} denotes constraints on the global positions of other joints:

$$\mathcal{L}_{\text{wr}} = \lambda_{\text{wr}} \sum_i \sum_{j \notin \text{arm}} \|P_{j,i} - P'_{j,i}\|_2^2. \quad (18)$$

The design of the smoothness loss is similar to Equation 13, penalizing huge acceleration of human SMPL-X parameters to avoid great motion differences between frames:

$$\mathcal{L}_{\text{smooth}} = \lambda_{\text{smooth}} \sum_i \sum_{j \in \{1,2\}} (a_{\theta_{j,i}})^2 + (a_{T_{j,i}})^2 + (a_{O_{j,i}})^2. \quad (19)$$

To leverage contact constraints, we attract human hands to the corresponding contact region on *target*. We select the positions of 20 fingertips of the two persons in the i -th frame as $\mathcal{H}_i = \{P_{\text{tip},i}\}_{\text{tip} \in [1,20]}$, where \bar{P} are tip positions in the object’s coordinate system. The contact vertices on the *target* from object-centric contact retargeting are defined as $\mathcal{C} = \{\bar{P}'_{\text{tip}}\}_{\text{tip} \in [1,20]}$. We minimize the Chamfer Distance (CD) between \mathcal{H}_i and \mathcal{C} to obtain contact consistency:

$$\mathcal{L}_c = \lambda_c \sum_i CD(\mathcal{H}_i, \mathcal{C}). \quad (20)$$

The total human motion retargeting problem is:

$$\theta_{1,2}, T_{1,2}, O_{1,2} \leftarrow \underset{\theta_{1,2}, T_{1,2}, O_{1,2}}{\text{argmin}} (\mathcal{L}_j + \mathcal{L}_c + \mathcal{L}_{\text{spat}} + \mathcal{L}_{\text{smooth}}), \quad (21)$$

In practice, we run 1,000 and 1,500 iterations respectively for object motion retargeting and human motion retargeting. The whole pipeline is implemented in PyTorch with Adam solver. The learning rate is 0.01. In object motion retargeting, λ_f for rotation is 500, for translation is 0.005, $\lambda_{\text{spat}} = 0.01$, $\lambda_{\text{smooth}} = 1$. In human motion retargeting, $\lambda_{\text{sr}} = 0.1$, $\lambda_{\text{wr}} = 0.003$, $\lambda_c = 1,000$, $\lambda_{\text{spat}} = 0.01$, and $\lambda_{\text{smooth}} = 1$.

C.4 Human-centric contact selection

The pairwise training dataset utilized for the human pose discriminator training comprises 636,424 pairs of data. Each pair encompasses a positive human pose $S_{\text{pos}} \in \mathbb{R}^{21 \times 3}$ and a negative human pose $S_{\text{neg}} \in \mathbb{R}^{21 \times 3}$. The positive human pose is sampled from the CORE4D-Real. Conversely, the negative human pose is derived from the corresponding positive sample by introducing noise to its object pose, subsequently employing the original contact information to perform contact-guided interaction retargeting. The discriminator is trained by:

$$\mathcal{L}_{\text{ranking}} = -\log(\sigma(R_{\text{pos}} - R_{\text{neg}} - m(S_{\text{pos}}, S_{\text{neg}}))), \quad (22)$$

iterating 1,000 epochs by the Adam solver with a learning rate $2e-4$.

Specifically, the noise $\Delta(\alpha, \beta, \gamma, x, y, z)$ incorporates both rotational and translational components. The rotational noise $\Delta(\alpha, \beta, \gamma)$ ranges from 20 to 60 degrees, while the translational noise $\Delta(x, y, z)$ falls within the range of 0.2 to 0.5 meters. The margin is computed by:

$$m(S_{\text{pos}}, S_{\text{neg}}) = (|\alpha| + |\beta| + |\gamma|)/10 + (|x| + |y| + |z|) * 10. \quad (23)$$

During the contact constraint update process, a penetration filtering step is performed. For each frame, the penetration volume between the human and object is calculated. If the penetration volume exceeds 10^{-4} cubic meters, it is considered a penetration case. If more than 2.5% of frames within an interaction candidate exhibit penetration, the entire candidate is discarded. Among the remaining candidates, the one with the highest score from the human pose discriminator is selected to proceed with the contact constraint update.

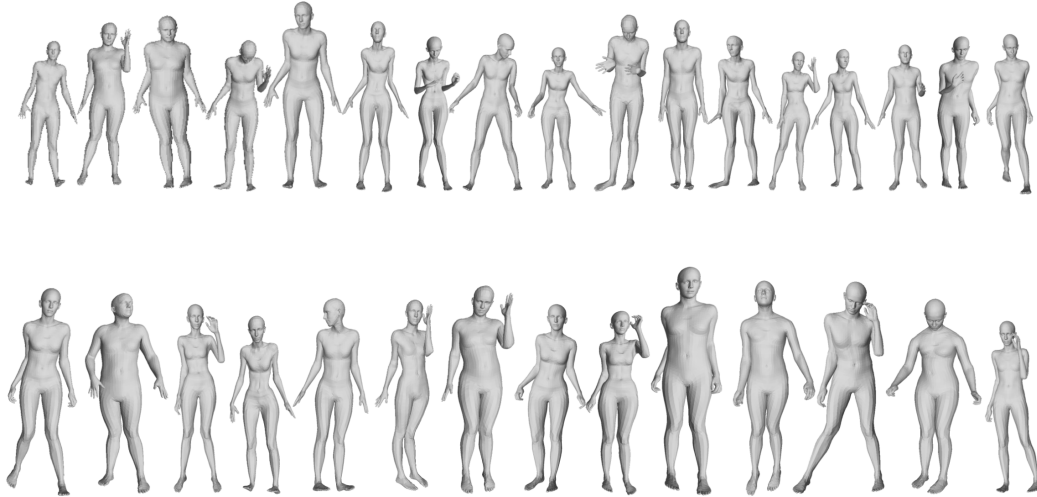


Figure 5: Visualization of all participants in CORE4D-Real.

Table 7: Statistics on object in CORE4D.

Set	#Object						#Sequence					
	Chair	Desk	Box	Board	Barrel	Stick	Chair	Desk	Box	Board	Barrel	Stick
Real	5	6	9	5	9	4	157	213	200	128	206	58
Synthetic	418	408	376	589	602	596	1767	1344	1326	2123	1495	1961

D Dataset Statistics and Visualization

D.1 Collaboration Modes

CORE4D encompasses five human-human cooperation modes in collaborative object rearrangement. “Move1” refers to the scenario where two participants simultaneously rearrange objects and both are aware of the target. On the other hand, “move2” represents the scenario where objects are rearranged simultaneously, but only Person 1 knows the target. “Pass” indicates that one participant passes the object to another for relay transportation. “Join” means that Person 2 joins Person 1 in carrying the object during transportation. Lastly, “leave” signifies that Person 2 leaves during the joint transportation with Person 1.

According to the different durations of the two participants’ contact with the object, “move1” and “move2” can be combined into collaborative carrying tasks. “Pass” represents the task of handover and solely moving the object. Incorporating the join task and the leave task, CORE4D totally comprises four different tasks (see Figure 4 in the main paper) based on the interaction between humans and objects. Fig. 10 exemplifies the motions for each task.

As depicted in Fig. 6, distinct characteristics are exhibited by different cooperation modes in high-level movements, thereby offering an innovative standpoint and potential for comprehending and investigating collaborative behaviors.

D.2 Participants

As illustrated in Fig. 5, a total of 31 participants, encompassing variations in height, weight, and gender, contributed to the capturing of CORE4D-Real.

D.3 Objects

CORE4D-Real has 38 objects while CORE4D-Synthetic has about 3k objects. The objects encompass six categories, namely box, board, barrel, stick, chair, and desk, each exhibiting a rich diversity in surface shape and size. The distribution of object categories is detailed in Table 7. All the objects

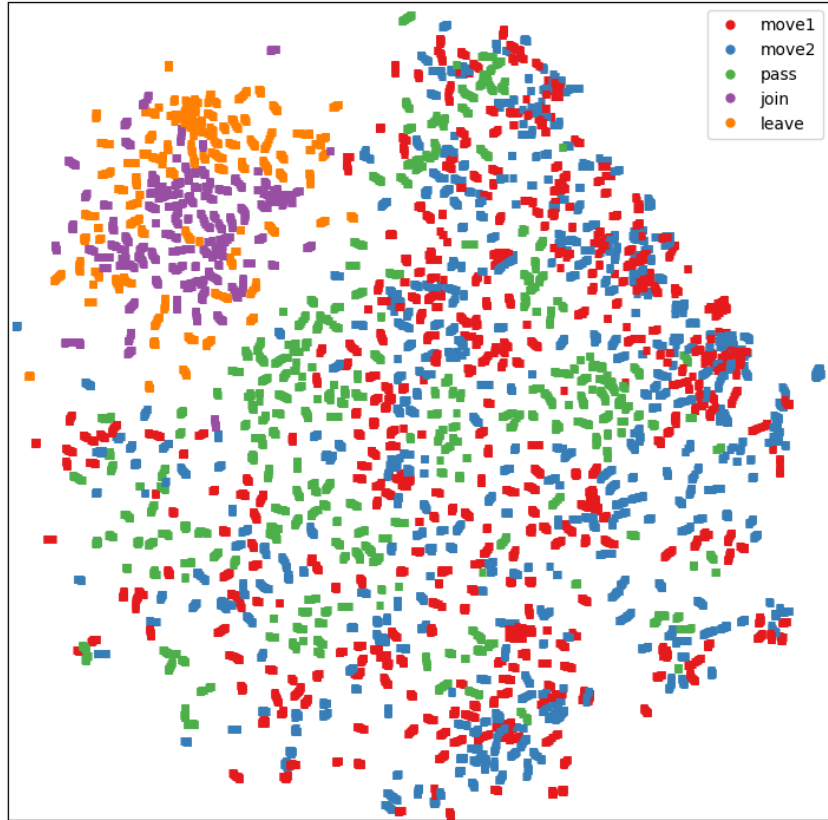


Figure 6: T-SNE visualization of human poses for different collaboration modes.

in CORE4D-Real are shown in Fig. 9. Fig. 8 shows samples from CORE4D-Synthetic and their interpolation process.

D.4 Camera Views

Fig. 7 shows the four allocentric and one egocentric views of our data capturing system.

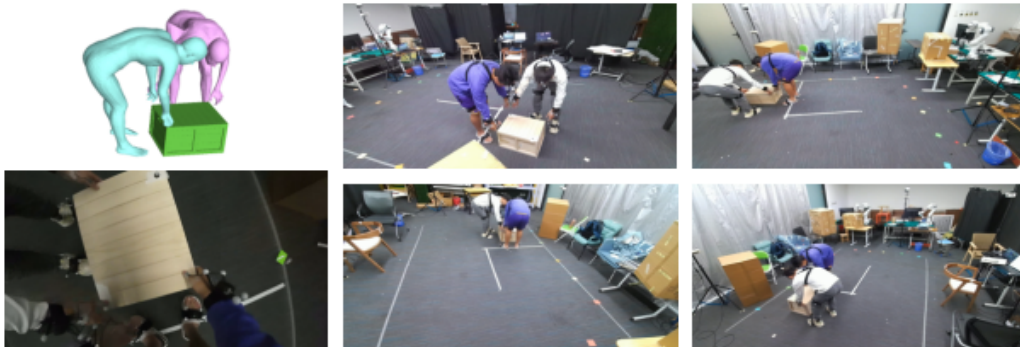


Figure 7: Visualization of CORE4D camera views.

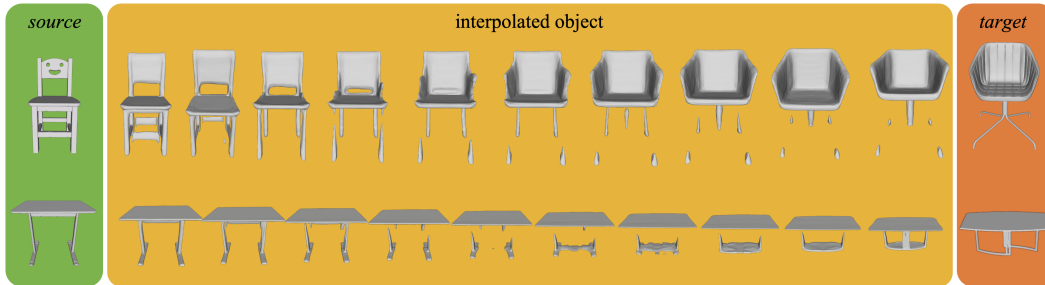


Figure 8: **Visualization of CORE4D-Synthetic objects and interpolation.**

Table 8: **Train-test split on CORE4D.**

Set	#Object						#Sequence					
	Chair	Desk	Box	Board	Barrel	Stick	Chair	Desk	Box	Board	Barrel	Stick
T-Real	3	4	6	3	6	2	93	104	96	51	113	25
T-Synthetic	418	408	376	589	602	596	1767	1344	1326	2123	1495	1961
S1	3	4	6	3	6	2	40	62	45	21	51	6
S2	2	2	3	2	3	2	24	47	59	56	42	27

E Details on Data Split

Benefiting from the diverse temporal collaboration patterns from CORE4D-Real and the large data amount of CORE4D-Synthetic, we randomly select a subset of real object models and construct the training set as the combination of their real (T-Real) and synthesized (T-Synthetic) collaboration motion sequences. We formulate two test sets on CORE4D-Real supporting studies of both non-generalization and inner-category generalization. The first test set (S1) consists of interaction performed on the objects that appear in the training set, while the second one (S2) is composed of interaction from novel objects. Detailed data distribution of each object category is shown in Table 8.

F Evaluation Metrics for Benchmarks

The code of our evaluation metrics is provided in Code Repository.

F.1 Human-object Motion Forecasting

Evaluation metrics include the human joints position error J_e , the object translation error T_e , the object rotation error R_e , the human-object contact accuracy C_{acc} , and the penetration rate P_r .

- We define J_e as the average Mean Per Joint Position Error (MPJPE) of the two persons. MPJPE represents the mean per-joint position error of the predicted human joint positions and the ground-truth values.
- Translation error (T_e) and rotation error (R_e) denote the average L2 difference between the predicted object translation vectors and the ground-truth ones, and the average geodesic difference between the estimated object rotation matrices and the ground-truth ones, respectively.
- Physical metrics: To assess contact fidelity, we detect contacts on the two hands of the two persons for each frame with an empirically designed distance threshold (5 centimeters). We then examine the contact accuracy (C_{acc}), which indicates the average percentage of contact detection errors in the predicted motions. Additionally, we examine the object penetration ratio (P_r) representing the mean percentage of object vertices inside the human meshes.

F.2 Interaction Synthesis

Following an existing individual human-object interaction synthesis study[40], the evaluation metrics include the root-relative human joint position error $RR.J_e$, the root-relative human vertex position error $RR.V_e$, the human-object contact accuracy C_{acc} , and the FID score (FID).

- $RR.J_e$ denotes the average root-relative MPJPE of the two persons. The root-relative MPJPE represents the mean per-joint position error of the predicted human joint positions relative to the human root position and the ground-truth values.
- $RR.V_e$ denotes the average root-relative Mean Per Vertex Position Error (MPVPE) of the two persons. The root-relative MPVPE represents the mean per-vertex position error of the predicted human vertex positions relative to the human root position and the ground-truth values.
- C_{acc} is the same as that in Section F.1.
- The Fréchet Inception Distance (FID) quantitatively evaluates the naturalness of synthesized human motions. We first train a feature extractor on CORE4D-Real to encode each human-object-human motion sequence to a 256D feature vector \bar{f}_i and acquire the ground-truth human motion feature distribution $\bar{D}=\{\bar{f}_i\}$. We then replace the motions of the two persons as synthesized ones and obtain another distribution $D=\{f_i\}$. Eventually, the FID denotes the 2-Wasserstein distance between \bar{D} and D . Since CORE4D-Real provides action labels, the feature extractor is supervised-trained by fulfilling the action recognition task. The network structure of the feature extractor is a single-layer Transformer[75]. We provide the code of the feature extractor and pre-trained parameters in Code Repository.

G Qualitative Results on Benchmarks

Figure 11 and Figure 12 exemplify generated motions for the human-object motion forecasting task and the interaction synthesis task, respectively, where ‘‘GT’’ denotes the ground truth motions, and others are method predictions. Since the baseline methods do not focus on generating hand poses, we replace hand poses in ground truth with flat hands to facilitate fair comparisons. Despite diverse cooperation modes that can be generated, the baseline methods consistently encompass unsatisfactory performances including unnatural collaboration, inter-penetration, and unnatural contact.

H Details on the Application of CORE4D-Synthetic

To evaluate the application of CORE4D-Synthetic, we use the lightweight CAHMP[14] to conduct the motion forecasting experiments. Unlike the experiments in section **Human-object Motion Forecasting** mentioned in the main paper, where 15 frames are predicted, here we predict the human-object motion for the next 10 frames given the previous 10 frames.

H.1 Task Formulation

Given the object’s 3D model and human-object poses in adjacent 10 frames, the task is to predict their subsequent poses in the following 10 frames. The human pose $P_h \in \mathbb{R}^{23 \times 3}$ represents the joint rotations of the SMPL-X[61] model, while the object pose $P_o = \{R_o \in \mathbb{R}^3, T_o \in \mathbb{R}^3\}$ denotes 3D orientation and 3D translation of the rigid object model.

H.2 Evaluation Metrics

Following existing motion forecasting works[12, 78, 88], we evaluate human joints position error J_e , object translation error T_e , object rotation error R_e . Details of the three metrics can be found in Section F.1.

H.3 Results

Comparing the 1K real dataset with the 0.1K real dataset supplemented with synthetic data generated through retargeting, we observed that the quality of the synthetic data is comparable to the real data. Additionally, due to the increased diversity of objects and enriched spatial relations between humans and objects in the synthetic data, it exhibits better generalization performance in object motion forecasting.

Comparing the evaluation results of the 1K real dataset with the results obtained by augmenting it with additional 4K synthetic data, we observed a significant performance gain from the synthetic data. This demonstrates that the inclusion of synthetic data enhances the value of our dataset and better supports downstream tasks.

I CORE4D-Real Data Capturing Instructions and Costs

I.1 Instructions.

Target. We divide a $4m \times 5m$ field into 20 squares and number them, and place colored labels as markers along the perimeter of the field. The following language instructs participants: *"Please collaboratively move the object to the target square. You can choose any path and orientation of the object as you like. It is not necessary to be overly precise with the final position - a rough placement is fine. Do not make unnatural motions just to achieve an exact position. Do not use verbal communication with each other."* As for the settings when only one participant knows the target, the target square number is written on a piece of paper and shown to the participant who knows the target. And additional instructions are given as: *"If you know the target, do not use language or direct body language to inform the other party (such as pointing out the location). If you do not know the target, please assist the other participant in completing the transportation."*

Collaboration Mode. The instructions are given as follows to indicate different Collaboration Modes for the participants. For Collaborate mode: *"Based on the target, please cooperatively transport the object, or upright any overturned tables, chairs, etc. Both participants should be in contact with the object throughout the process."* For Handover mode: *"Please decide the handover point yourselves, then have one person hand the object to the other, completing the object transfer in relay."* For Leave and Join modes: *"One person will transport the object throughout, while the other leaves or joins to help at a time point not disclosed to the collaborator."*

Obstacle. The instructions are given as follows to guide the participants in tackling obstacles: *"There are a varying number of obstacles on the field. If they get in your way, please decide on your own how to solve it using some common everyday operations. If the obstacles occupy the destination, please place the object near the destination."*

I.2 Costs.

Scanning the object took 30 person-hours, modeling the object into the mocap system took 27.5 person-hours, data capture took 78 person-hours, data annotation took 7 person-hours, and the user study took 60 person-hours. The wage is 100 RMB per person-hour.

J Experiment Configurations and Codes

We evaluate existing methods for the two benchmarks on Ubuntu 20.04 with one NVIDIA GeForce RTX 3090 GPU. The code of benchmarks and relevant methods are provided in Code Repository. During the quantitative evaluation, we select three random seeds (0, 42, 233) for each method, train the network respectively, and then report the mean performances and standard deviations as the evaluation results. More experimental details are provided in Code Repository.

K URLs of Dataset, Repository, Metadata, DOI, and License

- **Dataset project page:** <https://core4d.github.io/>.
- **Data link:** OneDrive Repository Link.
- **Dataset usage instruction:** <https://github.com/leolyliu/CORE4D-Instructions>.
- **Code link:** <https://github.com/leolyliu/CORE4D-Instructions>.
- **Croissant metadata:** Croissant Metadata Link.
- **Schema.org metadata:** <https://core4d.github.io/>.
- **DOI:** 10.5281/zenodo.11607666.
- **License.** This work is licensed under a CC BY 4.0 license.

L Dataset Documentation and Intended Uses

We use the documentation framework from *Gebru et.al*[21].

L.1 Motivation

- For what purpose was the dataset created? Was there a specific task in mind? Was there a specific gap that needed to be filled? Please provide a description.

The dataset was created to facilitate research studies in multi-person collaboration for object rearrangement. The dataset can support various research topics for understanding and synthesizing collaborative behaviors, including human-object motion tracking, action recognition, human-object motion forecasting, and collaboration synthesis.

- Who created the dataset (e.g., which team, research group) and on behalf of which entity (e.g., company, institution, organization)?

The dataset was created by Chengwen Zhang from Beijing University of Posts and Telecommunications, together with Yun Liu, Ruofan Xing, Bingda Tang, and Li Yi from Tsinghua University.

- Who funded the creation of the dataset? If there is an associated grant, please provide the name of the grantor and the grant name and number.

Funding was provided by the Institute for Interdisciplinary Information Sciences at Tsinghua University.

- Any other comments?

None.

L.2 Composition

- What do the instances that comprise the dataset represent (e.g., documents, photos, people, countries)? Are there multiple types of instances (e.g., movies, users, and ratings; people and interactions between them; nodes and edges)? Please provide a description.

The dataset comprises two parts: CORE4D-Real and CORE4D-Synthetic. The CORE4D-Real includes 3D object models, human-object motions, allocentric RGBD videos, egocentric RGB videos, human-object segmentations, camera parameters, and action labels. The CORE4D-Synthetic includes 3D object models and human-object motions. Please refer to the Dataset Documentation for explicit definitions of these files.

- How many instances are there in total (of each type, if appropriate)?

CORE4D-Real includes 37 object models, 1.0K human-object motion sequences, 4.0K allocentric RGBD videos, 1.0K egocentric videos, 4.0K human-object segmentations, and 1.0K action labels. CORE4D-Synthetic includes 3.0K object models and 10K human-object motion sequences.

- Does the dataset contain all possible instances or is it a sample (not necessarily random) of instances from a larger set? If the dataset is a sample, then what is the larger set? Is the sample representative of the larger set (e.g., geographic coverage)? If so, please describe how this representativeness was validated/verified. If it is not representative of the larger set, please describe why not (e.g., to cover a more diverse range of instances, because instances were withheld or unavailable).

The dataset is a representative sample of all possible and infinitely many multi-human collaborative behaviors for household object rearrangement. To cover as diverse collaboration as possible, we collect five typical collaboration modes in the CORE4D-Real, and enrich human-object spatial relations greatly in the CORE4D-Synthetic. Each collaboration sequence is complete.

- What data does each instance consist of? “Raw” data (e.g., unprocessed text or images) or features? In either case, please provide a description.

For CORE4D-Real, each collaboration instance consists of SMPLX[61] models of two persons in each frame, the 3D model for the manipulated object, the object’s 6D pose in each frame, four allocentric RGBD videos with camera intrinsic and extrinsic, one egocentric RGB video with the camera intrinsic, four human-object segmentation sequences, and one action label. For CORE4D-Synthetic, each collaboration instance consists of SMPLX[61] models of two persons in each frame, the 3D model for the manipulated object, and the object’s 6D pose in each frame. Details are provided in Dataset Documentation.

- Is there a label or target associated with each instance? If so, please provide a description.
For CORE4D-Real, each collaboration instance is associated with an action label. There is no label in CORE4D-Synthetic.
- Is any information missing from individual instances? If so, please provide a description, explaining why this information is missing (e.g., because it was unavailable). This does not include intentionally removed information, but might include, e.g., redacted text.
No information is missing.
- Are relationships between individual instances made explicit (e.g., users' movie ratings, social network links)? If so, please describe how these relationships are made explicit.
Relationships between individual collaboration instances include the same persons or the same objects. We provide an explicit SMPLX[61] shape parameter for each person, and an explicit name and 3D object model for each object.
- Are there recommended data splits (e.g., training, development/validation, testing)? If so, please provide a description of these splits, explaining the rationale behind them.
The recommended data split is provided in Code Repository.
- Are there any errors, sources of noise, or redundancies in the dataset? If so, please provide a description.
Noises come from the hardware noises of the inertial-optical mocap system, the 3D scanner, and the cameras.
- Is the dataset self-contained, or does it link to or otherwise rely on external resources (e.g., websites, tweets, other datasets)? If it links to or relies on external resources, a) are there guarantees that they will exist, and remain constant, over time; b) are there official archival versions of the complete dataset (i.e., including the external resources as they existed at the time the dataset was created); c) are there any restrictions (e.g., licenses, fees) associated with any of the external resources that might apply to a dataset consumer? Please provide descriptions of all external resources and any restrictions associated with them, as well as links or other access points, as appropriate.
The dataset is fully self-contained.
- Does the dataset contain data that might be considered confidential (e.g., data that is protected by legal privilege or by doctor-patient confidentiality, data that includes the content of individuals' nonpublic communications)? If so, please provide a description.
No confidential data.
- Does the dataset contain data that, if viewed directly, might be offensive, insulting, threatening, or might otherwise cause anxiety? If so, please describe why.
No.
- Does the dataset identify any subpopulations (e.g., by age, gender)? If so, please describe how these subpopulations are identified and provide a description of their respective distributions within the dataset.
No.
- Is it possible to identify individuals (i.e., one or more natural persons), either directly or indirectly (i.e., in combination with other data) from the dataset? If so, please describe how.
No. We ensure participants' anonymity by mosaicking their faces.
- Does the dataset contain data that might be considered sensitive in any way (e.g., data that reveals race or ethnic origins, sexual orientations, religious beliefs, political opinions or union memberships, or locations; financial or health data; biometric or genetic data; forms of government identification, such as social security numbers; criminal history)? If so, please provide a description.
No.
- Any other comments?
None.

L.3 Collection Process

- How was the data associated with each instance acquired? Was the data directly observable (e.g., raw text, movie ratings), reported by subjects (e.g., survey responses), or indirectly inferred/derived from other data (e.g., part-of-speech tags, model-based guesses for age or language)? If the data was reported by subjects or indirectly inferred/derived from other data, was the data validated/verified? If so, please describe how.

The data is acquired by the method described in Section 3 of the main paper. The data quality is evaluated in Section A and Section 4.4 of the main paper.

- What mechanisms or procedures were used to collect the data (e.g., hardware apparatuses or sensors, manual human curation, software programs, software APIs)? How were these mechanisms or procedures validated?

The data is collected by the method described in Section 3 of the main paper. The hardware qualities of the inertial-optical mocap system, the 3D scanner, and the cameras are examined by their developers.

- If the dataset is a sample from a larger set, what was the sampling strategy (e.g., deterministic, probabilistic with specific sampling probabilities)?

The dataset is a representative sample of all possible and infinitely many multi-human collaborative behaviors for household object rearrangement. To cover as diverse collaboration as possible, we collect five typical collaboration modes in the CORE4D-Real, and enrich human-object spatial relations greatly in the CORE4D-Synthetic. The dataset is not a sample from a known larger set since each motion sequence is complete.

- Who was involved in the data collection process (e.g., students, crowdworkers, contractors) and how were they compensated (e.g., how much were crowdworkers paid)?

Students from Universities participated in the data collection process. They were paid 100 RMB/hour. Thanks to them all.

- Over what timeframe was the data collected? Does this timeframe match the creation timeframe of the data associated with the instances (e.g., recent crawl of old news articles)? If not, please describe the timeframe in which the data associated with the instances was created.

The data was created and collected between July 2023 and December 2023. The creation time and the collection time of each data instance are the same.

- Were any ethical review processes conducted (e.g., by an institutional review board)? If so, please provide a description of these review processes, including the outcomes, as well as a link or other access point to any supporting documentation.

No.

- Did you collect the data from the individuals in question directly, or obtain it via third parties or other sources (e.g., websites)?

The data is the individuals' motions.

- Were the individuals in question notified about the data collection? If so, please describe (or show with screenshots or other information) how notice was provided, and provide a link or other access point to, or otherwise reproduce, the exact language of the notification itself.

Yes. The language is: "As a data collector, you will be familiar with the working principle and usage of the optical-inertial hybrid motion capture system. You will personally wear the motion capture device to collect motion data. All the data collected in this project will be used solely for research purposes by the Yili Research Group at Tsinghua University's Institute for Interdisciplinary Information Sciences."

- Did the individuals in question consent to the collection and use of their data? If so, please describe (or show with screenshots or other information) how consent was requested and provided, and provide a link or other access point to, or otherwise reproduce, the exact language to which the individuals consented.

Yes. All the participants signed that: "I am aware of and agree that the collected data will be used for research purposes related to the project and may be released as a dataset."

- If consent was obtained, were the consenting individuals provided with a mechanism to revoke their consent in the future or for certain uses? If so, please provide a description, as well as a link or other access point to the mechanism (if appropriate).

Yes. All participants were notified that they have the right to request the removal of their data at any time in the future by reimbursing their salary and compensating for the expenses incurred in collecting their data.

- Has an analysis of the potential impact of the dataset and its use on data subjects (e.g., a data protection impact analysis) been conducted? If so, please provide a description of this analysis, including the outcomes, as well as a link or other access point to any supporting documentation.

No.

- Any other comments?

None.

L.4 Preprocessing/cleaning/labeling

- Was any preprocessing/cleaning/labeling of the data done (e.g., discretization or bucketing, tokenization, part-of-speech tagging, SIFT feature extraction, removal of instances, processing of missing values)? If so, please provide a description. If not, you may skip the remaining questions in this section.

No.

- Was the “raw” data saved in addition to the preprocessed/cleaned/labeled data (e.g., to support unanticipated future uses)? If so, please provide a link or other access point to the “raw” data.

N/A

- Is the software that was used to preprocess/clean/label the data available? If so, please provide a link or other access point.

N/A

- Any other comments?

None.

L.5 Uses

- Has the dataset been used for any tasks already? If so, please provide a description.

Currently, the dataset has been used to establish two benchmarks, human-object motion forecasting and interaction synthesis, in Section 4 of the main paper.

- Is there a repository that links to any or all papers or systems that use the dataset? If so, please provide a link or other access point.

Yes. Please refer to Relevant Works.

- What (other) tasks could the dataset be used for?

The dataset can support various research topics for understanding and synthesizing collaborative behaviors, including human-object motion tracking, action recognition, human-object motion forecasting, and collaboration synthesis. Besides, the dataset can potentially be further used to study robot policies for robot manipulations and human-robot collaborations.

- Is there anything about the composition of the dataset or the way it was collected and preprocessed/cleaned/labeled that might impact future uses? For example, is there anything that a dataset consumer might need to know to avoid uses that could result in unfair treatment of individuals or groups (e.g., stereotyping, quality of service issues) or other risks or harms (e.g., legal risks, financial harms)? If so, please provide a description. Is there anything a dataset consumer could do to mitigate these risks or harms?

Unknown to the authors.

- Are there tasks for which the dataset should not be used? If so, please provide a description.

Unknown to the authors.

- Any other comments?

None.

L.6 Distribution

- Will the dataset be distributed to third parties outside of the entity (e.g., company, institution, organization) on behalf of which the dataset was created? If so, please provide a description.
Yes. The dataset is fully released at Dataset Repository. The project page of the dataset is CORE4D Project Page.
- How will the dataset will be distributed (e.g., tarball on website, API, GitHub)? Does the dataset have a digital object identifier (DOI)?
The dataset is distributed on Yun Liu's OneDrive Cloud Storage: Dataset Repository.
DOI: <https://doi.org/10.5281/zenodo.11607666>.
Project page: CORE4D Project Page.
- When will the dataset be distributed?
The dataset is distributed in June 2024.
- Will the dataset be distributed under a copyright or other intellectual property (IP) license, and/or under applicable terms of use (ToU)? If so, please describe this license and/or ToU, and provide a link or other access point to, or otherwise reproduce, any relevant licensing terms or ToU, as well as any fees associated with these restrictions.
The dataset is licensed under a CC BY 4.0 license.
- Have any third parties imposed IP-based or other restrictions on the data associated with the instances? If so, please describe these restrictions, and provide a link or other access point to, or otherwise reproduce, any relevant licensing terms, as well as any fees associated with these restrictions.
No.
- Do any export controls or other regulatory restrictions apply to the dataset or to individual instances? If so, please describe these restrictions, and provide a link or other access point to, or otherwise reproduce, any supporting documentation.
No.
- Any other comments?
None.

L.7 Maintenance

- Who will be supporting/hosting/maintaining the dataset?
Chengwen Zhang is supporting/maintaining the dataset.
- How can the owner/curator/manager of the dataset be contacted (e.g., email address)?
The curators of the dataset, Chengwen Zhang, Yun Liu, Ruofan Xing, Bingda Tang, and Li Yi, can be contacted at zcwoctopus@gmail.com, yun-liu22@mails.tsinghua.edu.cn, xingrf20@mails.tsinghua.edu.cn, tbd21@mails.tsinghua.edu.cn, and ericyi@mail.tsinghua.edu.cn, respectively.
- Is there an erratum? If so, please provide a link or other access point.
No.
- Will the dataset be updated (e.g., to correct labeling errors, add new instances, delete instances)? If so, please describe how often, by whom, and how updates will be communicated to dataset consumers (e.g., mailing list, GitHub)?
The dataset update will be posted at Dataset Instructions and CORE4D Project Page.
- If the dataset relates to people, are there applicable limits on the retention of the data associated with the instances (e.g., were the individuals in question told that their data would be retained for a fixed period of time and then deleted)? If so, please describe these limits and explain how they will be enforced.
No.
- Will older versions of the dataset continue to be supported/hosted/maintained? If so, please describe how. If not, please describe how its obsolescence will be communicated to dataset consumers.

After a dataset update, older versions will be kept for consistency. These notices will be posted at Dataset Instructions and CORE4D Project Page.

- [If others want to extend/augment/build on/contribute to the dataset, is there a mechanism for them to do so? If so, please provide a description. Will these contributions be validated/verified? If so, please describe how. If not, why not? Is there a process for communicating/distributing these contributions to dataset consumers? If so, please provide a description.](#)

Others are allowed to do these and should contact the original authors.

- [Any other comments?](#)
None.

M Author Statement

Author Responsibility Statement

This statement is intended to emphasize the author's responsibility regarding the dataset work, including ensuring compliance with all relevant laws, regulations, and ethical guidelines. By participating in the dataset work, the author agrees and commits to the following responsibilities:

- **Legality:** The authors guarantee that all data and materials used in the dataset work are obtained and used legally. The authors will ensure compliance with all applicable laws, regulations, and policies within their country, region, or organization.
- **Rights Protection:** The authors will make every effort to protect the privacy rights, intellectual property rights, and other legitimate interests of individuals within the dataset. The authors will respect individuals' privacy and take appropriate measures to safeguard the security of personal identifying information.
- **Transparency:** The authors will provide sufficient information and explanations to enable users of the dataset to understand the sources, purposes, and limitations of the data. The authors will strive to ensure that the use and publication of the dataset are transparent and traceable.
- **Compliance:** The authors will ensure that the dataset work complies with all applicable laws, regulations, and policies. In the event of any violation of rights, the authors will bear full responsibility and be willing to accept the corresponding legal consequences and liability for damages.
- **Shared Responsibility:** The authors require others who use the dataset to also assume appropriate responsibilities and adhere to similar obligations and guidelines to ensure the legal and responsible use of the dataset.
- **License Confirm:** This work is licensed under a CC BY 4.0 license.

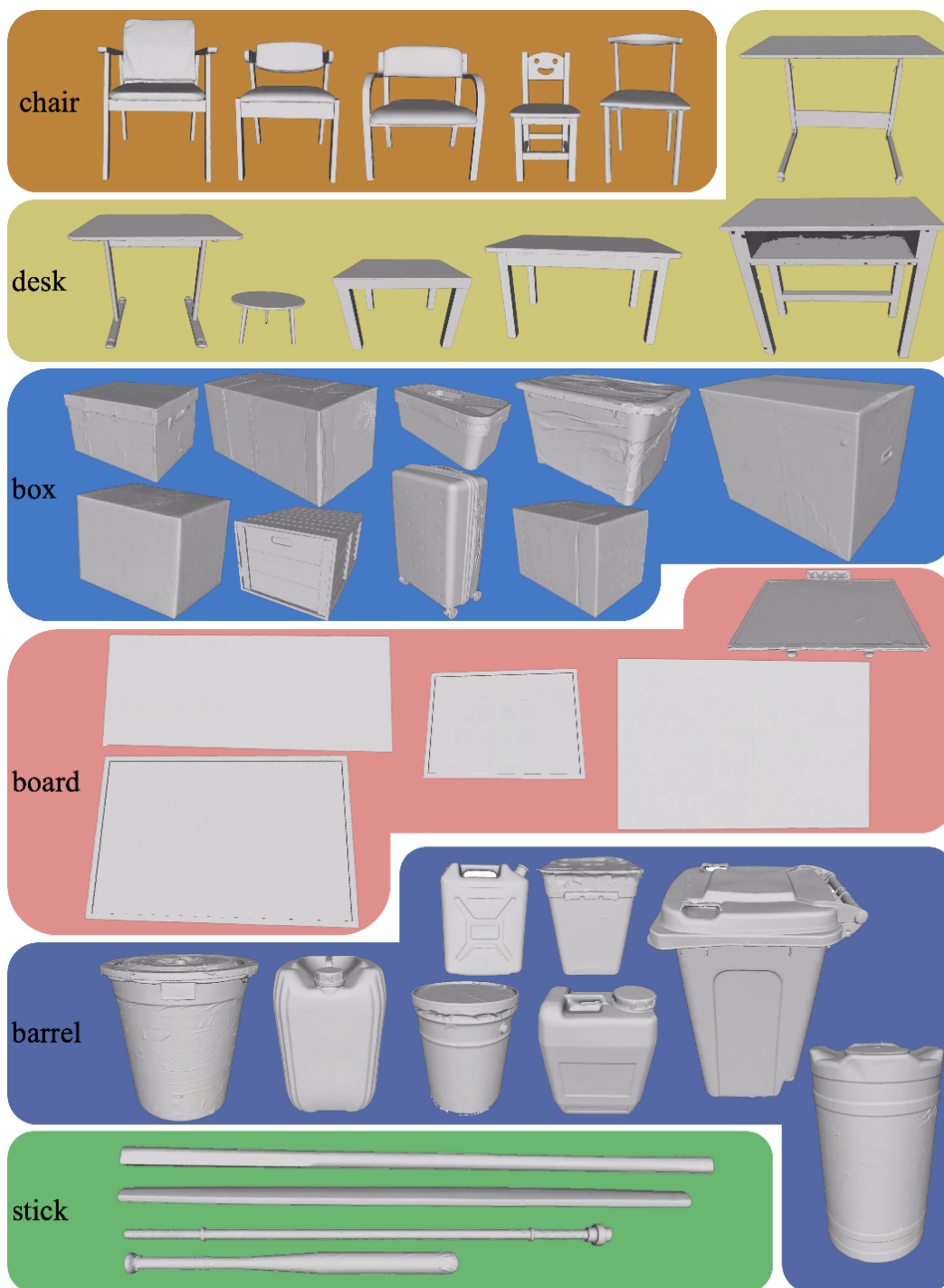


Figure 9: Visualization of CORE4D-Real objects.

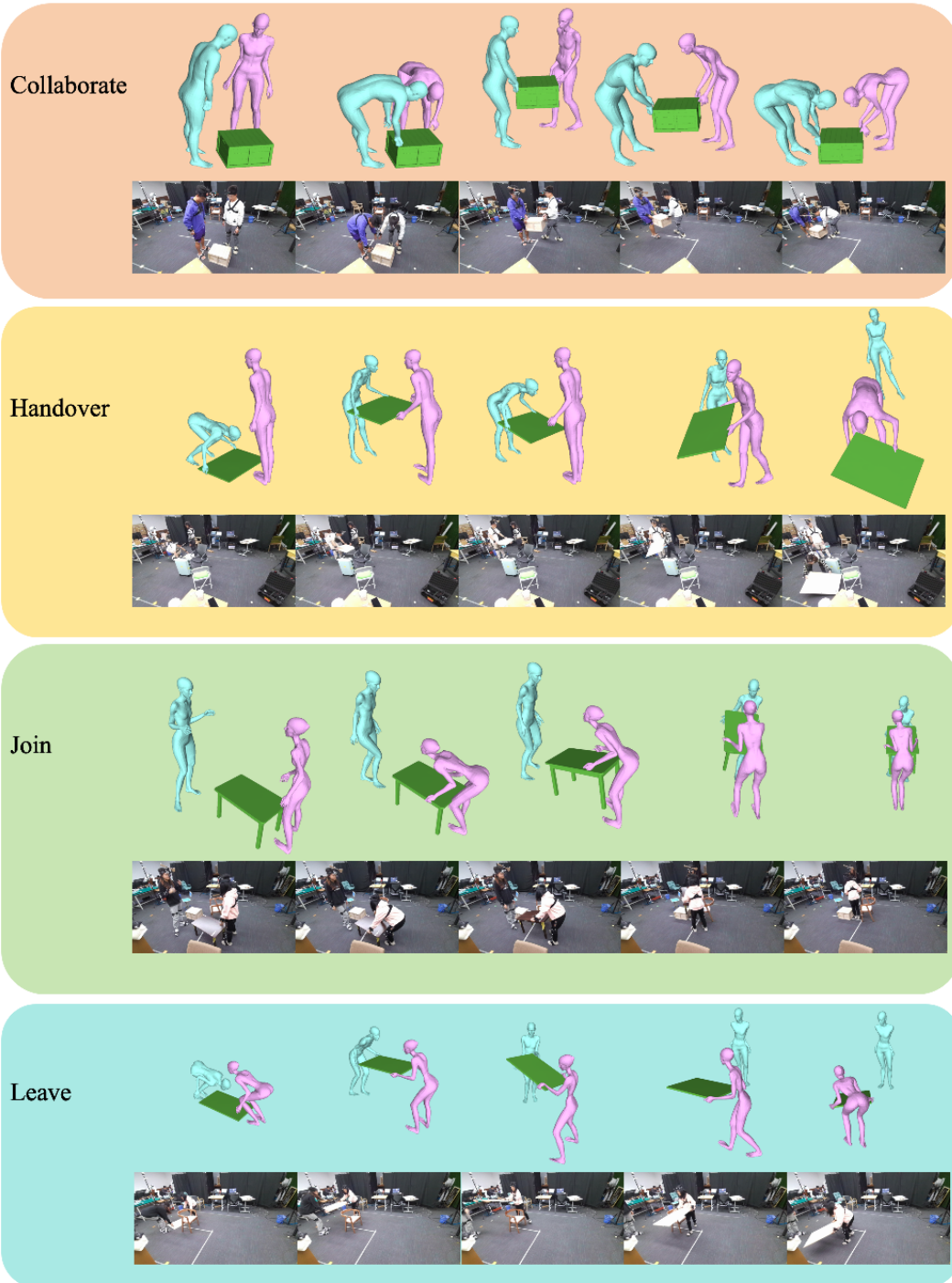


Figure 10: Visualization of CORE4D object rearrangement tasks.

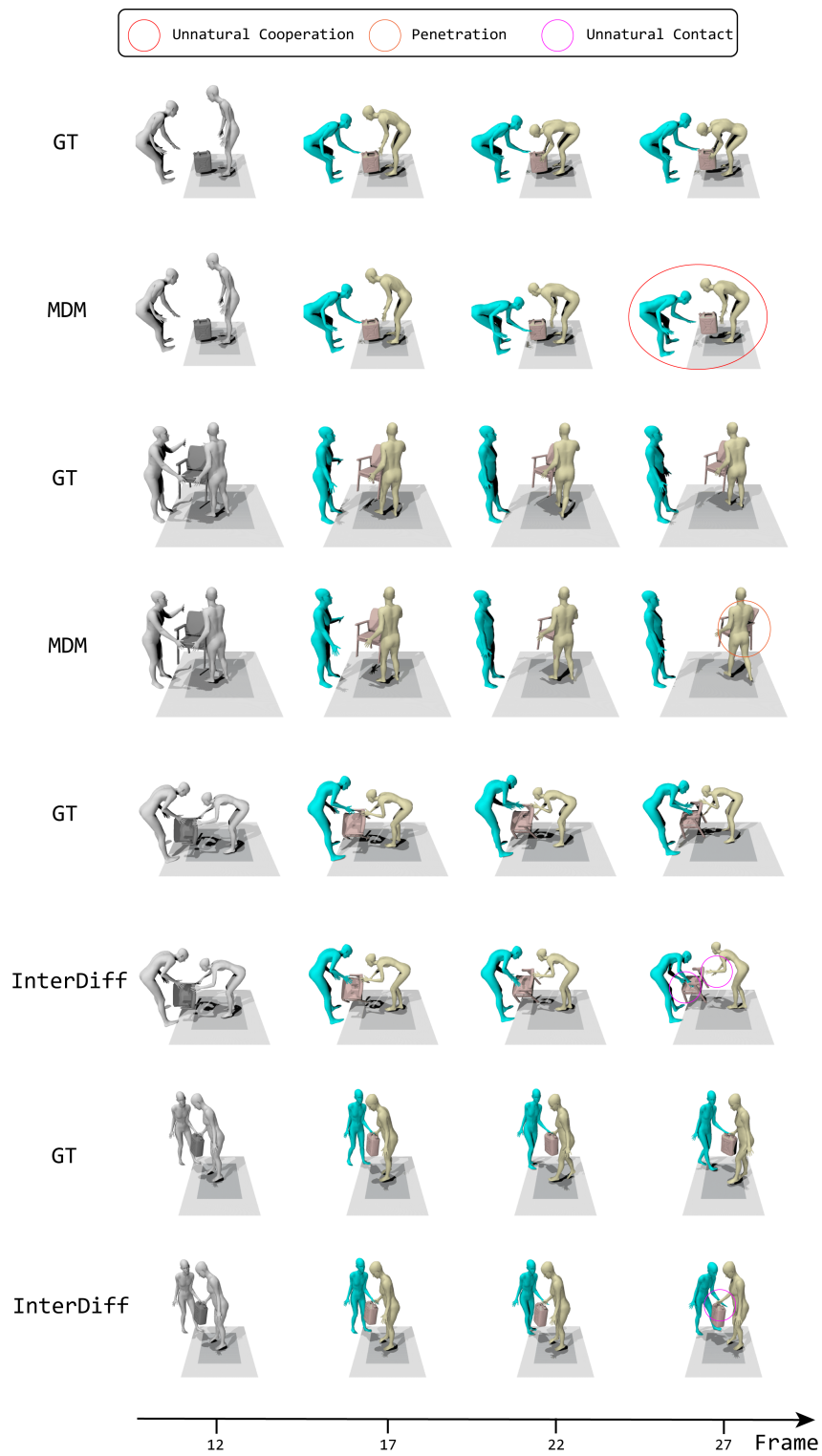


Figure 11: **Qualitative results of human-object motion forecasting.** Grey meshes are from the task inputs.

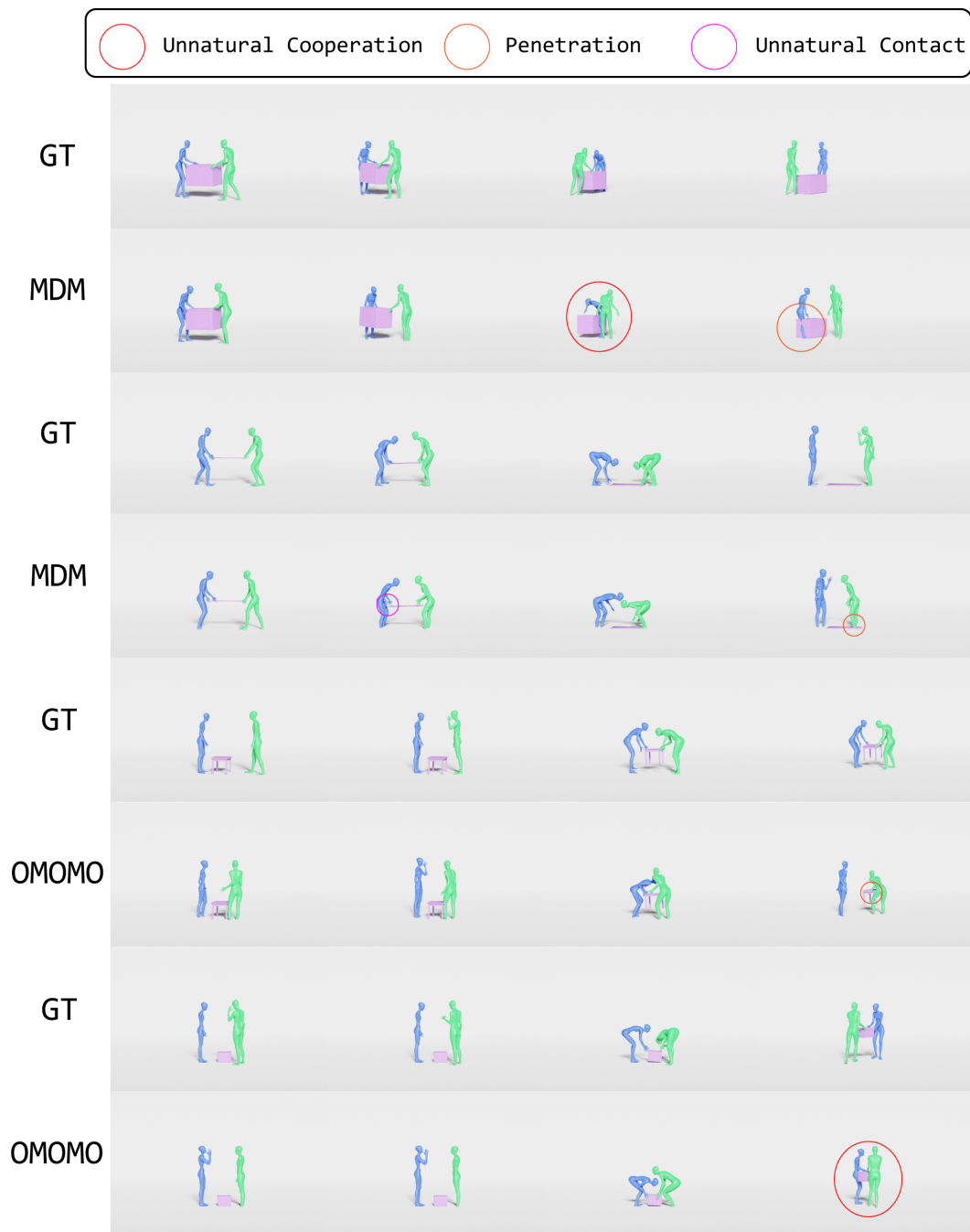


Figure 12: **Qualitative results of interaction synthesis.**